

# A Comparative Study of Palmprint Recognition Algorithms

DAVID ZHANG, The Hong Kong Polytechnic University / Harbin Institute of Technology  
WANGMENG ZUO and FENG YUE, Harbin Institute of Technology

2

Palmprint images contain rich unique features for reliable human identification, which makes it a very competitive topic in biometric research. A great many different low resolution palmprint recognition algorithms have been developed, which can be roughly grouped into three categories: holistic-based, feature-based, and hybrid methods. The purpose of this article is to provide an updated survey of palmprint recognition methods, and present a comparative study to evaluate the performance of the state-of-the-art palmprint recognition methods. Using the Hong Kong Polytechnic University (HKPU) palmprint database (version 2), we compare the recognition performance of a number of holistic-based (Fisherpalms and DCT+LDA) and local feature-based (competitive code, ordinal code, robust line orientation code, derivative of Gaussian code, and wide line detector) methods, and then investigate the error correlation and score-level fusion performance of different algorithms. After discussing the achievements and limitations of current palmprint recognition algorithms, we conclude with providing several potential research directions for the future.

Categories and Subject Descriptors: A.1 [Introductory and Survey]; I.4 [Image Processing and Computer Vision]; I.5.4 [Pattern Recognition]: Applications

General Terms: Algorithms, Performance

Additional Key Words and Phrases: Biometrics, feature extraction, palmprint recognition, performance evaluation, person identification

## ACM Reference Format:

Zhang, D., Zuo, W., and Yue, F. 2012. A comparative study of palmprint recognition algorithms. *ACM Comput. Surv.* 44, 1, Article 2 (January 2012), 37 pages.  
DOI = 10.1145/2071389.2071391 <http://doi.acm.org/10.1145/2071389.2071391>

## 1. INTRODUCTION

With the increasing demand of biometric solutions for security systems, palmprint recognition, a relatively novel but promising biometric technology, has recently received considerable interest [Duta et al. 2002; Jain et al. 2004; Shu and Zhang 1998; Zhang 2004; Zhang and Shu 1999]. Palmprints (the inner surface of the palm) carry several kinds of distinctive identification features for accurate and reliable personal recognition. Like fingerprints, palmprints have permanent discriminative features, including patterns of ridges and valleys, minutiae, and even pores in high resolution (>1000dpi) images [Cummins and Midlo 1961; SWGFAST 2006]. Aside from these

---

The work is partially supported by the GRF fund from the HKSAR Government, the central fund from the Hong Kong Polytechnic University, and the NSFC/SZHK funds under Contract Nos. 60902099 and SG200810100003A.

Authors' addresses: D. Zhang, Biometrics Research Centre, Department of Computing, Hong Kong Polytechnic University, Kowloon, Hong Kong/Shenzhen University, Harbin Institute of Technology, Shenzhen, China; email: csdzhang@comp.polyu.edu.hk; W. Zuo and F. Yue, School of Computer Science and Technology, Harbin Institute of Technology, Harbin, China; email: wzmzuo@hit.edu.cn.

Permission to make digital or hard copies of part or all of this work for personal or classroom use is granted without fee provided that copies are not made or distributed for profit or commercial advantage and that copies show this notice on the first page or initial screen of a display along with the full citation. Copyrights for components of this work owned by others than ACM must be honored. Abstracting with credit is permitted. To copy otherwise, to republish, to post on servers, to redistribute to lists, or to use any component of this work in other works requires prior specific permission and/or a fee. Permissions may be requested from the Publications Dept., ACM, Inc., 2 Penn Plaza, Suite 701, New York, NY 10121-0701, USA, fax +1 (212) 869-0481, or [permissions@acm.org](mailto:permissions@acm.org).

© 2012 ACM 0360-0300/2012/01-ART2 \$10.00

DOI 10.1145/2071389.2071391 <http://doi.acm.org/10.1145/2071389.2071391>

quasi fingerprint features, palmprints also carry other particular distinctive features, including principal lines and wrinkles.

In Jain and Feng [2009], the discriminative palmprint features are grouped into two subclasses: ridges and creases. In Jain et al. [2007], ridge features are further divided into three levels: Level 1 (ridge pattern), Level 2 (minutia points), and Level 3 (pores and ridge contours). Level 1 and Level 2 features can be extracted from fingerprint or palmprint images with 500 or less dpi, while Level 3 features should be extracted from 1000 dpi images. For ridge-based palmprint recognition, various Level 1 and Level 2 feature extraction and matching techniques developed for fingerprint recognition can be directly adopted. Minutiae extraction and descriptor are also proposed by taking the characteristics of latent palmprint into account [Jain and Demirkus 2008; Jain and Feng 2009]. Recently, the discriminative power of Level 3 features has been noticed by the biometric and forensics communities. Jain et al. [2007] have developed a hierarchical matching system to utilize Level 3 features for performance improvement in fingerprint matching. Although the acquisition and processing time of the high resolution palmprint images may restrict its applications in online personal authentication systems, ridge features are crucial for latent palmprint recognition, which has shown great potential in forensics and law enforcement.

Creases, also referred to as palm lines, include principal lines and wrinkles, which are obvious structural human features adopted for use in palmprint identification. The principal lines and some main wrinkles are formed several months after conception, and the other wrinkles are formed as the consequence of both genetic effects and various postnatal factors. The complex patterns of creases carry rich information for personal authentication. Most creases could be acquired with a low resolution scanner (100 dpi). Subsequently, online capture devices were developed to collect low resolution palmprint images in real time. Nowadays, low resolution palmprint recognition has gradually become a focus of research interest in the field of palmprint recognition [Li et al. 2002; Zhang et al. 2003]. In order to develop effective feature representation approaches, rather than explicitly extracting palm lines, low resolution palmprint images can also be treated as texture images, and texture descriptors are then used to describe invariant palmprint features.

With the rapid progress in sensor techniques and increase of computational power, except for low resolution palmprint recognition, several novel palmprint recognition technologies have been recently developed.

- (1) *Multispectral palmprint recognition.* Recent progress in multispectral imaging makes it possible to develop effective palmprint recognition methods by utilizing features obtained with different spectral wavelengths, such as visible, near infrared, infrared, and even single red, green, and blue channels [Han et al. 2008; Rowe et al. 2007; Zhang et al. 2010a]. With infrared spectral imaging, palm vein information would be captured to improve the capability of spoof detection and the accuracy of palmprint recognition. Another interesting direction is to pursue the optimal illumination (or lighting combination) for palmprint recognition by comparing and combining the recognition performance using whole visible spectral range light and light at several typical spectral bands. To date, several data-level, feature-level, and score-level fusion methods have been developed for multispectral palmprint recognition [Hao et al. 2007, 2008; Rowe et al. 2007].
- (2) *3D palmprint recognition.* 3D structural information on palm surface and lines also carries distinct discriminative features for personal authentication. Using a structured light vision technique, Zhang et al. [2010b] investigated 3D palmprint recognition by using mean curvature, Gaussian curvature, and surface type features. Compared with a 2D palmprint image, 3D depth information is difficult to

be imitated or disclosed, and thus 3D palmprint recognition is more robust against fake palmprint attack than 2D palmprint recognition [Zhang et al. 2009]. Since 2D information can also be acquired during 3D reconstruction, a high accuracy and robust palmprint recognition system could be constructed by combining 2D and 3D information.

- (3) *Latent palmprint recognition.* Latent palmprint is a crucial crime scene mark for suspect and victim identification in forensic applications. Different from low resolution palmprint recognition, latent palmprint recognition is a latent-to-full matching. Similar to fingerprint recognition, minutiae features and matching are usually adopted in latent palmprint recognition. Based on the characteristics of latent palmprints, Jain and Feng [2009] proposed a robust minutiae extraction method and a fixed-length minutia descriptor. Several local feature descriptors, e.g., the Scale Invariant Feature Transform (SIFT), have also been investigated in latent palmprint recognition [Jain and Demirkus 2008]. Regarding its important evidential value, latent palmprint recognition has shown great potential in forensics and law enforcement, such as the FBI's Next Generation Identification (NGI) system [NIST 2008], the British national palm print database and searching tool [CNET 2006].

In this article, we will concentrate on the survey of low resolution palmprint recognition algorithms. Regarding recent great progress in novel palmprint recognition techniques, in Section 2.2, we also provide an analysis and comparison of various local features for low resolution, latent, 3D, and multispectral palmprint recognition.

Building a palmprint recognition system usually involves four modules: image acquisition, preprocessing, feature extraction, and matching. In image acquisition, research teams have independently developed several CCD-based palmprint capture devices [Han 2004; Wong et al. 2005; Zhang et al. 2003, 2005]. Several public image databases have recently been released to facilitate the development of palmprint recognition technology.<sup>1,2,3</sup> In preprocessing, the aim is to detect several key points (usually two or more) to align different palmprint images and establish a reference coordinate system. According to the reference coordinate system, the central parts of palmprint images are segmented for subsequent feature extraction and matching [Dai et al. 2004; Li et al. 2002; Poon et al. 2004a; Zhang et al. 2003]. Rather than detecting the key points, some researchers suggested fitting an ellipse of the palmprint region, and then establishing the reference coordinate system in accordance with the orientation of the ellipse [Kumar et al. 2003].

In feature extraction and matching, a set of discriminative features is extracted from a palmprint image, and then compared against the stored templates to generate matching results. Feature extraction and matching are two of the most crucial problems in palmprint recognition, and have attracted researchers with different backgrounds, such as biometrics, pattern recognition, computer vision, and neural networks. Due to this fact, feature extraction and matching methods are much more diverse than preprocessing methods. In this article, palmprint feature extraction and matching algorithms are roughly grouped into three categories: holistic-based, feature-based, and hybrid methods. Holistic-based methods treat a palmprint image as an image, a high-dimensional vector, or a second rank tensor, and feature extraction and classification techniques are then used for palmprint recognition [Lu et al. 2003; Wu et al. 2003; Zuo et al. 2006b]. Feature-based methods extract local salient

<sup>1</sup>HKPU Palmprint Database, <http://www.comp.polyu.edu.hk/~biometrics/>.

<sup>2</sup>UST Hand Image Database, [http://visgraph.cs.ust.hk/biometrics/Visgraph\\_web/index.html](http://visgraph.cs.ust.hk/biometrics/Visgraph_web/index.html).

<sup>3</sup>CASIA Palmprint Database, <http://www.csbr.ia.ac.cn>.

features (such as edges, lines, and texture features) from palmprint images, and use a matcher to compare these against stored templates [Kong et al. 2003; Wu et al. 2004a, 2004b]. Hybrid methods use both holistic and local features to improve the recognition accuracy or facilitate identification speed [Kumar and Zhang 2005; Li et al. 2005a; You et al. 2004].

In the biometrics community, performance evaluation has received increasing attention. In recent years, the US National Institute of Standards and Technology (NIST) has conducted a number of excellent biometric evaluations in fingerprint, speaker, face, gait, and iris recognition [Doddington et al. 2000; Garris et al. 2006; Phillips 2007; Phillips et al. 2000, 2003; Sarkar et al. 2005]. In fingerprint recognition, from 2000 onwards, Cappelli et al. [2006] organized a series of famous independent competitions to evaluate state of the art fingerprint verification systems [Maio et al. 2002a, 2002b, 2004]. However, little work has been done on the comparative study of palmprint recognition algorithms. In this article, we first provide an updated survey of palmprint recognition methods, identify seven state of the art palmprint recognition methods, and then carry out a comparative study to evaluate the performance of these methods. More importantly, we intend to reveal the state of the art performance, identify the limitations of current palmprint recognition algorithms, and point out future directions for recognition algorithm development.

The remainder of this article is organized as follows. Section 2 presents a survey of current palmprint recognition algorithms. Section 3 briefly reviews several other topics on palmprint recognition, including complexity, partial recognition, sensing techniques, and antispoofing. Section 4 introduces seven palmprint recognition methods as well as the data set and performance indicators. Section 5 provides the experimental results, and discusses the memory and computational requirements. Section 6 studies the error correlation and score-level fusion performance of different methods. Finally, Section 7 draws some conclusions and identifies directions for future research.

## 2. SURVEY OF PALMPRINT RECOGNITION APPROACHES

With increasing interest in low resolution palmprint recognition, researchers have proposed a variety of palmprint feature extraction and matching approaches, which can be grouped into three categories: holistic-based, feature-based, and hybrid methods. In practice, sometimes it is difficult to distinguish feature extraction from matching, and thus we use the term “palmprint recognition approach” as a generalized denotation of a palmprint feature extraction and matching algorithm. In this section, we present a survey of these three categories of palmprint recognition approaches.

### 2.1 Holistic-Based Approaches

In the holistic-based palmprint recognition approach, the original palmprint image is used as the input of a holistic feature extractor or matcher (classifier), and thus there are two main issues, holistic palmprint image representation and classifier design. A summary of existing holistic palmprint recognition approaches is shown in Table I. In this section, we first survey several palmprint image representation methods in Section 2.1.1, and then summarize the classification methods in Section 2.1.2.

*2.1.1 Palmprint Image Representation.* Generally, palmprint images can be represented either in a spatial or a transform domain. On one hand, holistic palmprint features can be extracted from the spatial domain by treating a palmprint image as a vector, two-dimensional matrix, or second order tensor. On the other hand, using image transform techniques, holistic palmprint features can also be extracted from the transform domain.

Table I. Holistic-Based Palmprint Recognition Approaches

Approach	Representative work
(1) Holistic feature extraction	
(1.1) Subspace method	
Unsupervised linear method	Applications of PCA [Lu et al. 2003; Ribaric and Fratric 2005], ICA [Connie et al. 2003], and other unsupervised subspace methods [Yang et al. 2007]
Supervised linear method	PCA+LDA on raw data [Wu et al. 2003]
Kernel method	Applications of kernel PCA [Ekinici and Aykut 2007] and kernel Fisher discriminant [Wang and Ruan 2006b]
Tensor subspace method	Two-dimensional PCA [Zuo et al. 2006b], two-dimensional LPP [Hu et al. 2007]
Transform domain subspace method	Subspace methods in the transform domains [Jing and Zhang 2004; Jing et al. 2005]
(1.2) Invariant moment	Zernike moments [Li et al. 2005b] and Hu invariant moments [Noh and Rhee 2005]
(1.3) Spectral representation	
Wavelet signature	Global statistical signatures in wavelet domain [Zhang and Zhang 2004]
Correlation filter	Advanced correlation filter [Hennings et al. 2005; Hennings-Yeomans et al. 2007]
(2) Classifier design	
(2.1) Nearest neighbor	Extensively adopted in palmprint recognition [Hu et al. 2007; Jing and Zhang 2004; Jing et al. 2005, 2007; Yang et al. 2007; Yao et al. 2007]
(2.2) SVM	SVM with Gaussian kernel [Chen and Xie 2007]
(2.3) Neural network	Backpropagation neural network [Han et al. 2003], modular neural network [Zhao et al. 2007]

According to spatial palmprint representation, different holistic approaches are proposed for palmprint recognition. By treating a palmprint image as a two-dimensional image, several invariant image moments are extracted as the holistic palmprint feature [Li et al. 2005b]. By concatenating columns of a palmprint image into a high dimensional vector, varieties of linear and nonlinear subspace analysis technologies are applied to the palmprint feature extraction [Lu et al. 2003; Wu et al. 2003; Yang et al. 2007]. Most recently, by treating a palmprint image as a second order tensor, several tensor analysis approaches have been developed [Hu et al. 2007; Zuo et al. 2006b].

Different image transform techniques have been investigated for effective transform domain palmprint representation. The Fourier transform, a classical image transform technique, has been successfully applied to Fourier domain feature extraction and classifier design [Jing et al. 2005; Li et al. 2002]. Other image transform techniques, such as 2D Gabor transform and discrete cosine transform (DCT), can be combined with the subspace analysis method for efficient palmprint feature extraction [Jing and Zhang 2004; Jing et al. 2007; Pan et al. 2007a; Yao et al. 2007].

*2.1.2 Holistic Palmprint Feature Extraction.* The subspace method, invariant moments, and spectral representation are three main subclasses of holistic palmprint feature extraction approaches.

*2.1.2.1 Subspace Method.* The dimension of palmprint images is usually much higher than the number of available training samples, which is known as the small sample size (SSS) problem. To address the SSS problem, various unsupervised/supervised, vector/tensor, and linear/nonlinear subspace methods are proposed to map a palmprint image from the original data space to a lower-dimensional feature space [Zhang et al. 2006]. In the beginning, a linear unsupervised method—principal component analysis (PCA)—was used to extract the holistic feature vectors [Lu et al. 2003; Pan et al. 2007b; Ribaric and Fratric 2005]. Subsequently, other popular unsupervised methods, such as independent component analysis (ICA) and locality preserving projection (LPP), have been applied to palmprint recognition [Connie et al. 2003; Yang et al. 2007].

However, unsupervised subspace methods do not utilize class label information in the training stage, and supervised methods are thus generally expected to be more effective in dealing with recognition problems. Hence, Fisher’s linear discriminant analysis (LDA), which aims to find a set of the optimal discriminant vectors that map the original data into a low-dimensional feature space, has received considerable research interest. To address the SSS problem in supervised subspace methods, there are two popular strategies: transform-based and algorithm-based. The transform-based strategy, such as PCA+LDA, first transforms the original image data into a lower dimensional subspace and then uses LDA for feature extraction [Wu et al. 2003]. The algorithm-based strategy finds an alternative LDA formalization to circumvent the SSS problem [Jing et al. 2007; Qin et al. 2006].

Palmprint representation and recognition usually cannot be regarded as a simple linear problem. In the last few years, a class of nonlinear subspace methods—kernel-based subspace methods—was investigated for palmprint recognition. In the kernel-based method, data  $\mathbf{x}$  are implicitly mapped into a higher dimensional or infinite dimensional feature space  $\mathcal{F}$ :  $\mathbf{x} \rightarrow \Phi(\mathbf{x})$ ; the inner product in feature space can be easily computed using the kernel function  $K(\mathbf{x}, \mathbf{y}) = \langle \Phi(\mathbf{x}), \Phi(\mathbf{y}) \rangle$ . For the kernel trick, Schölkopf et al. [1998] pointed out that “every (linear) algorithm that only use scalar (inner) products can implicitly be executed in  $\mathcal{F}$  by using kernels, i.e. one can very elegantly construct a nonlinear version of a linear algorithm.” Now a number of kernel subspace methods, such as kernel PCA (KPCA) and kernel Fisher discriminant (KFD), have been applied for palmprint feature extraction [Aykut and Ekinici 2007; Ekinici and Aykut 2007; Wang and Ruan 2006b]. Most recently, another class of nonlinear dimensionality reduction technologies—manifold learning—with the corresponding linear and kernel formalizations, has also shown great potential in palmprint recognition [Hu et al. 2007; Wang et al. 2008; Yang et al. 2007].

A palmprint image can be treated as a tensor of order two, where tensor is a higher order generalization of a vector or matrix. With this formalization, a number of tensor subspace methods have been proposed. Most recently, motivated by two-dimensional PCA [Yang et al. 2004] and multilinear generalization of singular vector decomposition [Lathauwer et al. 2000], tensor analysis methods have been developed and applied to palmprint feature extraction [Hu et al. 2007; Wang and Ruan 2006a; Zuo et al. 2006a, 2006b].

Image transform can be used to further improve the performance of subspace methods. After image transform, the transform coefficients may be more effective for palmprint recognition and robust to within-class variation. Furthermore, using feature selection techniques, transform coefficients that are less discriminative may be excluded from subsequent processing operations and thus, total data dimensionality is efficiently reduced. Subspace methods have been successfully applied in the transform domains of several image transform techniques, such as Fourier [Jing et al. 2005],

Gabor [Ekinici and Aykut 2007], discrete cosine [Jing and Zhang 2004], and wavelet transform [Connie et al. 2003].

*2.1.2.2 Invariant Moments.* Image moments are capable of capturing global information of images, usually provide translation, rotation, or scale invariant properties, and thus, have found extensive applications in the field of image recognition. Using Zernike and Hu invariant moments, a number of feature descriptors have been developed for palmprint feature representation [Kong et al. 2008; Li et al. 2005b; Noh and Rhee 2005; Pang et al. 2004].

*2.1.2.3 Spectral Representation.* Using image transform, we can transform a palmprint image to its Fourier frequency transform domain, and then extract a set of frequency features or design a correlation classifier in the frequency domain to characterize palmprint discriminative features [Hennings et al. 2005; Ito et al. 2006; Li et al. 2002; Zhang and Zhang 2004]. Li et al. [2002] proposed using angular and radial energy information for palmprint representation. Zhang and Zhang [2004] first transformed a palmprint image into the wavelet domain, and then a set of global statistical signatures was extracted to characterize palmprint directional context features. Hennings et al. [2005] proposed training an advanced correlation filter in the Fourier transform domain for palmprint images from each palm. Furthermore, this group proposed using multiple correlation filters per class to enhance the accuracy of palmprint recognition [Hennings-Yeomans et al. 2007]. However, correlation filter is more likely to be a classification method rather than a feature extraction approach. Aside from correlation filter, there is another type of correlation method, known as phase-only matching [Ito et al. 2006].

*2.1.3 Classifier Design.* In palmprint recognition, a common characteristic is that the number of classes (palms) is much higher than the number of available samples of each class. In some cases, there is only one training image for each palm. Taking these factors into account, it would be difficult to estimate the hyper-parameters of sophisticated classifiers, and thus, the nearest neighbor classifier has been extensively adopted [Hu et al. 2007; Jing and Zhang 2004; Jing et al. 2005, 2007; Yang et al. 2007; Yao et al. 2007].

Other classification approaches, such as neural networks and support vector machine (SVM), have also been applied to palmprint recognition. In Chen and Xie [2007], SVM with Gaussian kernel is adopted for palmprint classification using dual-tree complex wavelet features. In Han et al. [2003], the backpropagation neural network is first applied to palmprint authentication. However, palmprint recognition is a typical large-scale multiclass problem, which is very difficult for backpropagation neural networks. In Li et al. [2005b; Zhao et al. 2007], the modular neural network is used to decompose the palmprint recognition task into a series of smaller and simpler two-class subproblems. In Jing et al. [2007] and Jing and Wong [2006], the RBF neural network is suggested for palmprint recognition due to its computational simplicity and favorable classification capability. Most recently, other neural networks, such as hierarchical neural network and radial basis probabilistic neural network, have also been proposed for palmprint authentication [Kong et al. 2008; Shang et al. 2006].

## 2.2 Local Feature-Based Approaches

There are two classes of local features for palmprint recognition—ridges and creases—which can be extracted from high resolution and low resolution palmprint images, respectively. For completeness, we also discuss the 3D structure features and multi-spectral features of palm/palmprint. Table II lists the characteristics of local features

Table II. Characteristics of Local Features in Palmprint Recognition

Feature	Resolution	Collectability	Permanence	Distinctiveness	Circumvention	Latent Recognition
Principal lines	Low	High	High	Low	High	No
Wrinkles	Median	High	Median	High	High	No
Multispectral	Low	Median	High	High	Low	No
3D	Median	Low	Median	Median	Median	No
Minutiae	High	Median	High	High	Median	Yes
Level 3	Very High	Low	Median	High	Low	Yes

in terms of acquisition resolution, collectability, permanence, distinctiveness, circumvention, and application in latent recognition. In the following, we briefly introduce the strength and restrictions of each kind of local palmprint features.

- (1) *Principal lines*. Compared with wrinkles, principal lines usually are the consequence of genetic effects, and thus have good permanence and are more significant in the palmprint images. The principal lines of twins are similar, which makes the distinctiveness of principal lines relatively low.
- (2) *Wrinkles*. Several wrinkles may only be stable for months or years. Thus the permanence of wrinkles is not as high as minutiae. Principal lines and wrinkles are difficult to be recovered from a crime scene, and almost no latent-to-full matching techniques are developed for principal line and wrinkle features, which makes principal lines and wrinkles less useful in latent recognition. A low resolution palmprint image has rich wrinkle information. By combining principal line and wrinkle features, we can establish a high performance online palmprint recognition system [Sun et al. 2005; Zhang et al. 2003].
- (3) *3D structure*. The acquisition of the 3D depth information of a palm surface is much more difficult than the acquisition of a 2D palmprint image. 3D palmprint recognition is robust against fake palmprint attack, and thus can be combined with 2D features to build a highly accurate and robust palmprint recognition system [Zhang et al. 2009, 2010b].
- (4) *Multispectral features*. Multispectral palmprint recognition utilizes features obtained with different spectral wavelengths/resolution/sensors for personal authentication [Rowe et al. 2007; Han et al. 2008; Hao et al. 2008]. Multispectral features can be regarded as an ensemble of palmprint features. Principal lines and wrinkles can be acquired at visible wavelengths, while palm veins can be acquired at infrared wavelengths. Since palm vein is difficult to be circumvented, multispectral features can be used to build a high accuracy and robust palmprint recognition system.
- (5) *Minutiae*. The distinctiveness and permanence of minutiae have been investigated in depth for fingerprint and palmprint recognition. Minutiae features can be extracted from palmprint images with 500 or less dpi, and are crucial for latent palmprint recognition. Recently, minutiae-based palmprint recognition has shown great potential in forensics and law enforcement [Jain and Demirkus 2008; Jain and Feng 2009].
- (6) *Level 3 features*. Level 3 features include all dimensional permanent attributes of the ridge, e.g., ridge path deviation, line shape, pores, edge contour, incipient ridges, warts, and scars [Jain et al. 2007]. Level 3 features play an important role in latent recognition, where 20 to 40 pores should be sufficient to determine the identity of a person [Ashbaugh 1999]. Currently, most Level 3 feature acquisition, extraction, and matching approaches are designed for fingerprint recognition.

In the remainder of this section, we will concentrate on the survey of local feature-based method for low resolution palmprint recognition. We do not take minutiae and

Table III. Local Feature-Based Palmprint Recognition Approaches

Approach	Representative work
(1) Line-based	
Derivatives of a Gaussian	First- and second-order derivatives of a Gaussian with different directions [Wu et al. 2006b]
Wide line detector	Extraction of the location and width information of palm line [Liu et al. 2007]
Line segment Hausdorff distance	Application of line segment Hausdorff distance [Gao and Leung 2002]
(2) Coding-based	
PalmCode	Coding of the phase of the 2D-Gabor filter responses [Zhang et al. 2003]
FusionCode	Coding of the phase of the 2D-Gabor filter responses with the maximum magnitude [Kong et al. 2006a]
Orientation code	Coding of the orientation information of palm lines [Jia et al. 2008; Kong and Zhang 2004; Sun et al. 2005]
(3) Palmprint texture descriptor	Local binary pattern [Wang et al. 2006], Coding of DCT coefficients [Kumar and Zhang 2006]

Level 3 feature extraction methods into account because they can only be extracted from high resolution palmprint images, and are usually used in latent recognition. Besides, several of the local feature-based methods could be extended for multispectral and 3D palmprint recognition [Rowe et al. 2007; Zhang et al. 2009].

Palm lines and texture are two kinds of local distinctive and stable features for low resolution palmprint authentication. A number of line detection approaches have been proposed to extract palm lines. However, several thin and weak palm lines, such as wrinkles, might be too vague for detection by a line detector. To avoid this, texture analysis approaches, such as coding-based methods and texture descriptors, have achieved great success in palmprint recognition. Thus, Table III summarizes the existing local feature-based approaches into three categories: line-based, coding-based, and texture descriptor methods.

*2.2.1 Line-Based Method.* To extract palm lines, Wu et al. [2006b] used the second-order derivatives of a Gaussian to represent the line magnitude, and the first-order derivatives of a Gaussian to detect the location of the line. The final result is obtained by combining all directional line detection results and then encoded using the chain code. To simultaneously extract the location and width information of palm lines, Liu et al. [2007] proposed a wide line detector using an isotropic nonlinear filter. Other methods, such as two-stage filtering, have also been applied to palm line detection [Wang and Ruan 2006c].

Another topic in the line-based method is local line matching, where a score is produced by matching two line images. An ordinary matching method is calculating the number (or proportion) of the line pixels that are in the same location as the two line images. However, the performance of this method would be unsatisfactory due to several unavoidable factors, such as the translation, rotation, and deformation of the palmprint images. To improve the line matching performance, Wu et al. [2006b] proposed dilating the template line image before matching, and Leung et al. [2007] used the line segment Hausdorff distance to denote the matching score of two line images [Gao and Leung 2002; Li and Leung 2006].

*2.2.2 Coding-Based Method.* The coding-based method encodes the response of a bank of filters into bitwise code. With the virtues of bitwise feature representation, a

coding-based method usually has a lower memory requirement and a fast matching speed, and thus has been very successful in palmprint representation and matching. Motivated by Daugman's IrisCode [Daugman 1993], Zhang and Kong developed a PalmCode method, which first convolved the palmprint image with a 2D Gabor filter, and then encoded the phase of the filter responses as bitwise features [Kong et al. 2003; Zhang et al. 2003]. However, the PalmCodes of different palms still have obvious correlations, and thus, might cause performance degradation of PalmCode. To improve the performance, Kong et al. [2006a] further introduced a FusionCode method, which convolves a palmprint image with a bank of Gabor filters with different orientations, and then encodes the phase of the filter response with the maximum magnitude.

Recent advances in coding-based methods indicate that the orientation information of palm lines is one of the most promising features for personal identification [Kong and Zhang 2004; Wu et al. 2006a]. Generally, there are three main topics in orientation coding: filter design, coding scheme, and matching approaches. In 2004, Kong and Zhang investigated the orientation coding problem, and proposed a competitive code method, where a bank of Gabor filters was utilized to extract the orientation information. A competitive coding scheme was used to generate a bitwise feature representation, and the angular distance was used to match two competitive codes [Kong and Zhang 2004]. Subsequently, other filters, such as elliptical Gaussian and Radon [Jia et al. 2008; Sun et al. 2005], other coding schemes, such as ordinal code [Sun et al. 2005] and integer coding [Jia et al. 2008; Wu et al. 2005], and other matching approaches, such as pixel to area comparison [Huang et al. 2008; Jia et al. 2008], have been developed for palmprint recognition.

*2.2.3 Local Palmprint Texture Descriptors.* A typical local palmprint texture descriptor usually divides a palmprint image (or a transformed image) into several small blocks, and then calculates the mean, variance, energy, or histogram of each block as local features [Han et al. 2007; Kumar and Zhang 2006; Wang et al. 2006; Wu et al. 2002]. Local binary pattern (LBP) [Ojala et al. 1996, 2002], a powerful texture analysis method, has been successfully applied to face recognition [Ahonen et al. 2004, 2006], and recently introduced to palmprint recognition through integration with AdaBoost [Wang et al. 2006]. Kumar and Zhang [2006] divided a palmprint image into overlapped blocks, calculated the DCT coefficients of each block, and used its standard deviation to form a feature vector. Other texture descriptors, such as directional element energy and local direction histogram, have also been adopted in palmprint recognition [Han et al. 2007; Wu et al. 2002].

*2.2.4 Other Methods.* With the exception of these three categories of local feature-based methods, there are several other algorithms, which are difficult to classify. For example, motivated by the success of the complex wavelet structural similarity index (CW-SSIM) in image quality evaluation [Wang et al. 2004], Zhang et al. [2007] proposed a modified CW-SSIM method for calculating the matching score of two palmprint images.

### 2.3 Hybrid Approaches

It has been argued that the human vision system uses both holistic and local features to recognize the object of interest, and hybrid approaches are thus expected to be promising for palmprint recognition. Hybrid approaches have two main applications: high accuracy palmprint recognition and fast palmprint matching, as shown in Table IV. Using both holistic and local feature-based methods to obtain a multiple palmprint representation, several feature-level, score-level, and decision-level fusion strategies can then be used to further improve recognition performance [Kittler et al.

Table IV. Hybrid Palmprint Recognition Approaches

Approach	Representative work.
Multiple palmprint representation (high accuracy)	Fusion of three palmprint representations, Gabor, line, and subspace features [Kumar and Zhang 2005]
Hierarchical matching scheme (fast matching)	Coarse-to-fine matching of palmprint features [Li et al. 2005a; You et al. 2004]

1998]. Following this criterion, a number of multiple palmprint representation approaches have been suggested [Kong et al. 2008; Kumar and Zhang 2005; Poon et al. 2004b]. For example, Kumar extracted three major palmprint representations: Gabor, line, and subspace features, and proposed a product of sum rule to combine their matching scores [Kumar and Zhang 2005].

Another important application of hybrid approaches is fast palmprint matching, where a hierarchical scheme is used for coarse-to-fine matching [Li et al. 2004a; You et al. 2002, 2005]. In You et al. [2004], the global geometry feature (Level-1), global texture energy (Level-2), fuzzy line feature (Level-3), and local texture energy feature (Level-4) are extracted to feed to a hierarchical classifier. During palmprint verification or identification, You et al. proposed using a guided search scheme to facilitate efficient palmprint matching. The scheme begins with matching of the simplest Level-1 feature. If the Level-1 matching distance is smaller than the predefined threshold  $T_1$ , matching of the next feature level is then performed until the Level- $i$  matching distance is smaller than a predefined threshold  $T_i$  or the matching of Level-4 feature is performed. Most hierarchical matching approaches are based on global geometry, lines, and texture features [Li et al. 2002, 2005a; You et al. 2004]. Only a few papers reported the use of pure global or local line features for constructing hierarchical classifiers [Li and Leung 2006].

### 3. OTHER TOPICS ON PALMPRINT RECOGNITION

In this section, we present a brief survey of several other palmprint recognition topics. Based on the categorization introduced in Section 2, we first compare the complexity and template size of different algorithms, then provide a survey of palmprint recognition methods for partial recognition and different sensing techniques, and finally review the anti-spoofing methods.

#### 3.1 Complexity and Template Size

Using the categorization introduced in Section 2, Table V provides a brief comparison of the palmprint recognition methods based on their complexity and template size. It should be noted that we evaluate the complexity and template size according to the state-of-the-art methods in each subclass, and do not take into account the methods with less complexity and small template size but with poor performance. Based on the characteristics of the methods, researchers may choose appropriate palmprint recognition methods to develop a system for a specific application and operation environment. For example, for a palmprint identification system used in a large enterprise, a hierarchical matching scheme can be adopted for fast personal identification, while a coding-based method would be appropriate for a real-time embedded verification system.

#### 3.2 Partial Palmprint Recognition

A real palmprint recognition system should capture, detect, and recognize a palmprint image automatically, making it inevitable that palmprint images will sometimes be only partially acquired. Some accessories, e.g., bandages, will also cause the partial occlusion of a palmprint image. Thus, the development of a palmprint authentication

Table V. Comparison of Various Palmprint Recognition Methods Based on Complexity and Template Size

Palmprint recognition methods	Computational complexity	Memory complexity	Template size
(1) Holistic methods			
Subspace method	Low	Medium	Medium
Invariant moment	Medium	Low	Low
Spectral representation	High	High	Medium
(2) Local feature-based methods			
Line-based	High	Medium	Medium
Coding-based	Medium	Low	Low
Texture descriptor	Medium	Medium	Medium
(3) Hybrid methods			
Multiple palmprint representation	High	High	High
Hierarchical matching scheme	Low	Medium	High

system should always address the robust recognition problem on a partially occluded or damaged palmprint image. If incorporated with palmprint quality evaluation methods, most coding-based methods, e.g., PalmCode [Zhang et al. 2003] and FusionCode [Kong et al. 2006a], can achieve robust recognition performance against partial occlusion or damage of palmprint images. Holistic methods, such as PCA and LDA, are robust in the presence of low levels of occlusion [Zhao et al. 2003]. However, if the degree of occlusion increases, the recognition performance would deteriorate severely. To address this, several robust appearance-based methods and sparse representation approaches have recently been developed for robust recognition against partially occluded or damaged images [Fidler et al. 2006; Wright et al. 2009; Zhang and Zuo 2007].

In latent palmprint recognition, the sample captured from crime scenes is always partial and incomplete, and minutiae features are usually adopted for latent-to-full matching based on the methodology used by latent experts. Conventional fingerprint recognition methods can be directly used for latent palmprint matching, but they may produce many spurious minutiae and fail in a palmprint area with dense thin creases. Jain and Feng [2009] proposed a latent palmprint matching system by using robust orientation field estimation, fixed-length minutia descriptor, and two-level minutiae matching. Local descriptors used in computer vision, e.g., SIFT, have also been investigated to facilitate latent-to-full palmprint matching [Jain and Demirkus 2008].

### 3.3 Algorithms for Different Sensing Techniques

In the last decade, visible, infrared, and 3D information acquisition techniques have been developed for online palmprint recognition. Based on the categorization introduced in Section 2, we present a brief summary of the application of holistic, local feature-based, and hybrid methods in visible, infrared, and 3D palmprint recognition, as shown in Table VI. Compared with low-resolution visible palmprint recognition, infrared and 3D palmprint acquisition techniques were developed in the latest few years, and to date only a small number of methods are reported for infrared and 3D palmprint recognition. Thus, it would be promising to use the experiences of visible palmprint recognition in future studies of palmprint recognition for other sensing techniques.

### 3.4 Antispoofing

A palmprint recognition system can be spoofed by fake palms, brute-force, replay, and other attacks. Kong et al. [2006b] studied the probabilistic model of brute-force

Table VI. Summary of the Application of Holistic-Based, Local Feature-Based and Hybrid Methods in Visible, Infrared, and 3D Palmprint Recognition

	Holistic method	Local feature-based method	Hybrid method
Visible	[Hennings-Yeomans et al. 2007; Lu et al. 2003; Wu et al. 2003]	[Kong and Zhang 2004; Liu et al. 2007; Sun et al. 2005; Zhang et al. 2003]	[Kumar and Zhang 2005; You et al. 2004]
Infrared	[Wang et al. 2008]	[Hao et al. 2007; Zhang et al. 2010a]	Not yet
3D	Not yet	[Zhang et al. 2010b]	Not yet

break-ins with projected multinomial distribution. Zhang et al. [2010b] investigated the performance degradation of 2D palmprint recognition caused by a faked palmprint attack, and proposed to use both 2D and 3D features to address this problem. In multispectral palmprint recognition, palm vein image captured with infrared spectral imaging can be used to improve the capability of spoof detection [Rowe et al. 2007; Zhang et al. 2010a]. From the security and privacy viewpoint, Connie et al. [2005] proposed a PalmHashing (also known as BioHashing) method by combining user-specific pseudo-random numbers (token) and palmprint features to generate cancelable palmprint representation, and reported zero equal error rates for face, fingerprint, and palmprint biometrics [Teoh et al. 2004]. It has been recognized, however, that the authentication performance of this method would be much poorer if the token is stolen [Kong et al. 2006; Teoh et al. 2008]. Recently, Kong et al. [2008] proposed a cancelable competitive code method to defend replay and database attacks.

## 4. DATA SET AND ALGORITHMS

### 4.1 Data Set

The HKPU palmprint database (version 2) is used to carry out a comprehensive comparison on the performance of several state-of-the-art palmprint recognition approaches. Compared with the UST hand image database and the CASIA palmprint database, the HKPU palmprint database is the largest that is publicly available and most extensively used in palmprint recognition research. The HKPU palmprint database consists of 7752 images captured from 386 palms of 193 individuals, where 131 people are male. The samples of each individual were collected in two sessions, where the average interval between the first and the second sessions was around two months. During each session, we captured about ten palmprint images each of the left and the right palms. The volunteers are mainly from the students and staff at the Hong Kong Polytechnic University, and the age distribution is: about 86 percent individuals younger than 30 years old, about 3 percent older than 50, and about 11 percent aged between 30 and 50. In the first session, we use a LED ring array over the spectral range from 380nm to 780nm and the focal length of the CCD camera is 8mm. To incorporate realistic intraclass variations, in the second session, we adjusted the focal length to 6mm and changed the light source to a ring-like incandescent lamp to approximate the CIE standard illuminant D65.

In our experiments, we first modified the preprocessing method described in Zhang et al. [2003] by fixing some minor problems, and then used it to crop each original palmprint image to a subimage to a size of 128×128. To ensure the credibility of the results, all the palmprint recognition algorithms were tested based on the same subimage set. Figure 1 shows two palmprint images and the corresponding cropped images of one palm, where the former image of Figure 1(a) is captured in the first session and the latter in the second session.

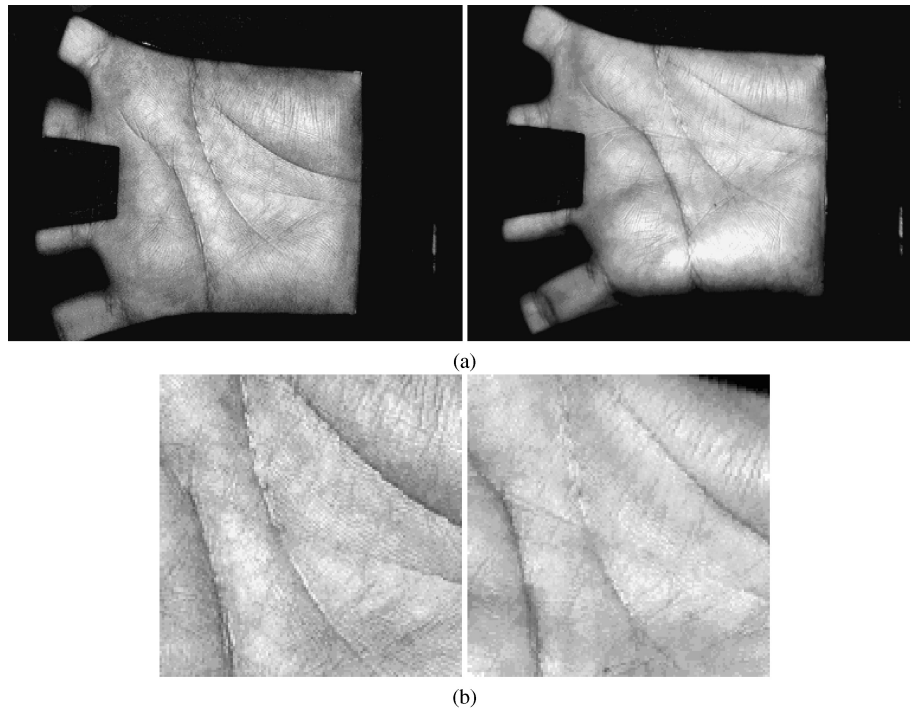


Fig. 1. Two images of a palm in the HKPU palmprint database: (a) original images, and (b) cropped images.

#### 4.2 Performance Indicators

Two groups of experiments were carried out to evaluate the verification and identification performance of each palmprint recognition algorithm. In palmprint verification, an input palmprint image is compared with a template to determine whether they are from the same palm. In our experiments, each of the palmprint images is compared with all remaining images. To evaluate the verification performance, the following performance indicators are used.

- *Genuine accept rate (GAR, %) vs. false acceptance rate (FAR, %) curve (GAR-FAR curve)*. GAR-FAR curve, a variant form of the receiver operating characteristic (ROC) curve, plots GAR against FAR for various decision thresholds, and has been very popular for performance evaluation of biometric systems.
- *Equal error rate (EER, %)*. The error rate at the specific threshold  $t$  for which  $(1-GAR)$  and FAR are equal;
- *GAR at a specific FRR ( $= 10^{-3}\%$ )*.  $GAR_{-3}$ .

In palmprint identification, an input palmprint image is compared with all the templates from the entire template set to determine the identity. In our experiments, for each palm, three palmprint images collected in the first session are used to construct a template set that contains 1158 images. For each test palmprint image, the minimum matching score generated by comparing the templates with the same palm is regarded as a genuine matching, and the minimum matching score generated by comparing the templates with a different palm is regarded as an imposter matching. We use the repeated random subsampling validation method to evaluate the identification performance and robustness of each algorithm. For each algorithm, in each run, we randomly select three samples of each subject in the first session to construct a template set, and

use the remaining samples in the first session as TestSet 1 (2731 samples) and all the samples in the second session as TestSet 2 (3863 samples). We then evaluate the identification rate of the algorithm on TestSet 1 and the identification rate on TestSet 2. We run this experiment 20 times and use the mean and standard deviation (*std.*) to denote the identification performance and robustness of the algorithm. To evaluate the identification performance, the following performance indicators are used.

- Identification rate (IR, %). the percentage of test images that are correctly recognized by a palmprint recognition algorithm;
- GAR-FAR curve (ROC curve);
- EER;
- GAR at a specific FRR (=  $10^{-2}\%$ ): GAR<sub>-2</sub>.

Finally, to evaluate the memory and computational requirements of each algorithm, the following performance indicators are used.

- Template size;
- Average feature extraction and matching time.

### 4.3 Palmprint Recognition Algorithms

We implemented seven palmprint recognition algorithms: competitive code, ordinal code, robust line orientation code (RLOC), derivative of the Gaussian (DoG) code, wide line detector, Fisherpalms, and DCT+LDA. In Cheung et al. [2006] and Kong [2007], Kong et al. carried out a comparison of several palmprint recognition approaches developed by our group, and showed that the competitive code would achieve higher verification accuracy in comparison to PalmCode, FusionCode, Eigenpalms, Fisherpalms, and so on.

**4.3.1 Competitive Code.** Competitive coding (CompCode) is an effective method for the extraction and representation of palm line orientation information [Kong and Zhang 2004]. The 2D Gabor function reformed by Lee [1996] is adopted for filtering the palmprint images. Furthermore, since palm lines are negative, we only used the negative real part of the 2D Gabor function.

$$\Psi(x, y, x_0, y_0, \omega, \theta, \kappa) = \frac{-\omega}{\sqrt{2\pi\kappa}} e^{-\frac{\omega^2}{8\kappa^2}(4x^2+y^2)} \left( \cos(\omega x') - e^{-\frac{\kappa^2}{2}} \right), \quad (1)$$

where  $x' = (x - x_0) \cos \theta + (y - y_0) \sin \theta$ ,  $y' = -(x - x_0) \sin \theta + (y - y_0) \cos \theta$ ,  $(x_0, y_0)$  is the center of the function,  $\omega$  is the radial frequency in radians per unit length, and  $\theta$  is the orientation of the Gabor functions in radians. The  $\kappa$  is defined by  $\kappa = \sqrt{2 \ln 2} \left( \frac{2^\delta + 1}{2^\delta - 1} \right)$ , where  $\delta$  is the half-amplitude bandwidth of the frequency response.

When  $\sigma$  and  $\delta$  are fixed,  $\omega$  can be derived from  $\omega = \kappa/\sigma$ .

Competitive code uses six 2D Gabor filters with orientations  $\theta_p = p\pi/6$ ,  $p = \{0, 1, \dots, 5\}$ , to generate a bitwise palmprint representation. Let  $I(x, y)$  denote the cropped subimage and  $\Psi(x, y, \theta)$  is the Gabor filter with orientation  $\theta$ . The competitive rule defined as.

$$j = \arg \min_{\theta} \{I(x, y) * \Psi(x, y, \theta)\} \quad (2)$$

is adopted to calculate the winning index  $j$ , where  $*$  denotes the convolution operator. After feature extraction, Kong and Zhang encoded each winning index into 3 bits for efficient palmprint representation. Figure 2 shows the procedure of the feature extraction and representation of competitive code.

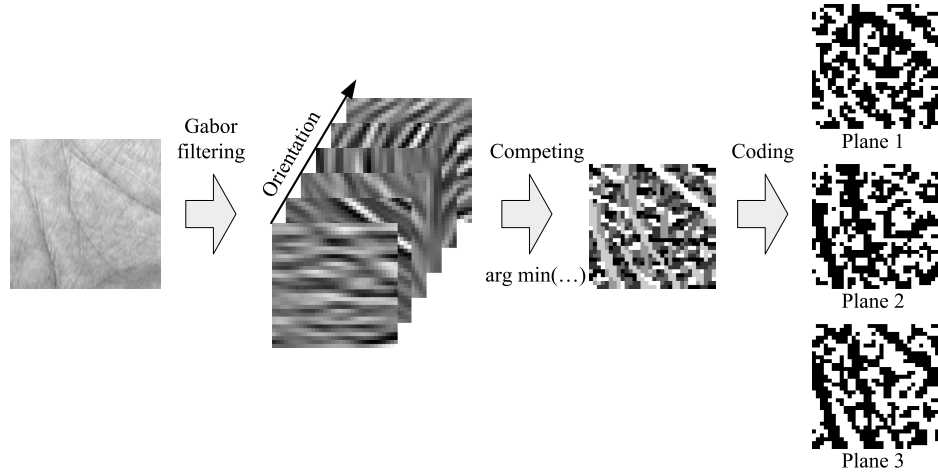


Fig. 2. Procedure of the competitive coding scheme.

In the matching stage, Kong and Zhang [2004] presented an angular distance based on Boolean operators. The distance between two palmprints is then defined as the summation of the angular distance of all sampling points. With the bitwise feature representation and angular distance, the distance (dissimilarity) between two competitive codes can be efficiently computed by employing Boolean operators.

**4.3.2 Ordinal Code.** Different from competitive code, ordinal code (OrdiCode) first uses six 2D elliptical Gaussian filters for filtering the palmprint image, and then compares each pair of filtering responses orthogonal in orientation to generate one bit feature code, [Sun et al. 2005]. The 2D elliptical Gaussian filter used by ordinal code is defined as

$$f(x, y, x_0, y_0, \delta_x, \delta_y, \theta) = \exp\left(-\left(\frac{x'}{\delta_x}\right)^2 - \left(\frac{y'}{\delta_y}\right)^2\right), \quad (3)$$

where  $x', y', x_0, y_0, \theta$  are the same as defined in Eq. (1),  $\delta_x$  and  $\delta_y$  are the horizontal and vertical scale of the Gaussian filter, respectively. Since this method only concerns the relative magnitude of the filtering responses orthogonal in orientation, Sun et al. [2005] proposed the ordinal coding rule as.

$$OF(x, y, \theta) = \frac{1 + \text{sgn}(I(x, y) * (f(x, y, \theta) - f(x, y, \theta + \pi/2)))}{2}, \quad (4)$$

where  $\text{sgn}(\cdot)$  is the sign function. The procedure of the feature extraction and representation of ordinal code is illustrated in Figure 3.

In terms of the code size, competitive code and ordinal code are the same. For each sampling point, the code length is three bits. In terms of the feature extraction speed, ordinal code scheme is much faster than competitive code. As shown in Eq. (4), the ordinal code can perform filter level combination. Thus, the filtering operation can be performed on only three orientations, which makes the ordinal code method save roughly half of the time for feature extraction in comparison to the competitive coding scheme.

**4.3.3 RLOC.** In the feature extraction stage, RLOC uses a modified finite Radon transform (MFRAT) to extract the orientation features of palm lines, and encodes the

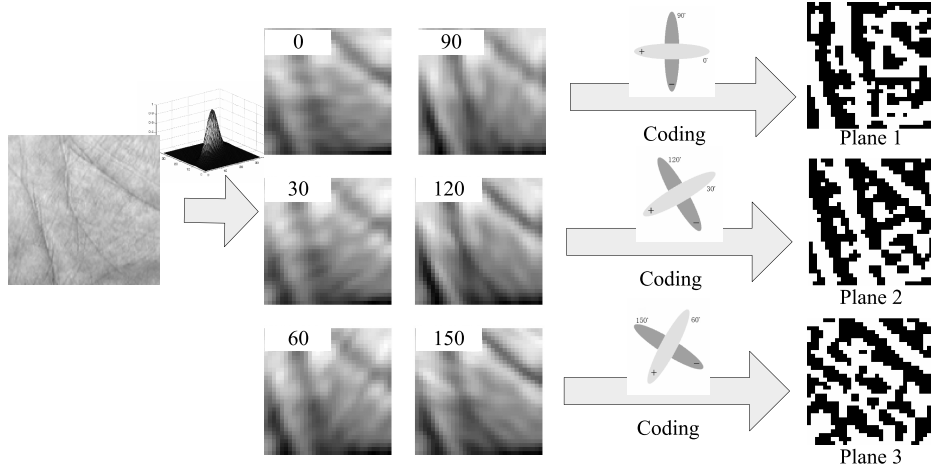
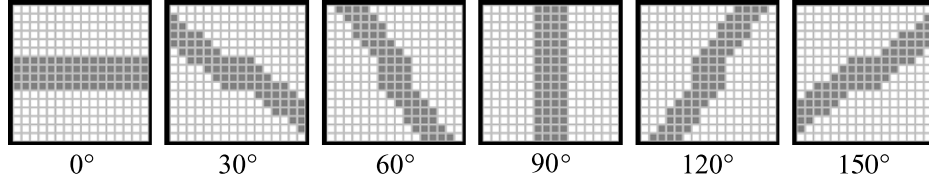


Fig. 3. Procedure of the ordinal coding scheme.

Fig. 4. The  $16 \times 16$  MFRAT templates [Jia et al. 2008].

winning orientation index [Jia et al. 2008]. Denoting  $Z_p = \{-p, \dots, 0, 1, \dots, p\}$ , where  $p$  is a positive integer, the MFRAT of an image  $I(i, j)$  on the finite grid  $Z_p^2$  is defined as

$$MFRAT_I(i_0, j_0, \theta) = \sum_{(i, j) \in L_\theta} I[i, j], \quad (5)$$

where  $L_\theta$  denotes the set of neighbor points of  $(i_0, j_0)$  that makes up a line with angle  $\theta_p = p\pi/6$ ,  $p = \{0, 1, \dots, 5\}$ , which means

$$L_\theta = \{(i, j) : i = l + i_0, j = k(i - i_0) + j_0, l \in Z_p\}, \quad (6)$$

where  $(i_0, j_0)$  denotes the center point, and  $k$  is the corresponding slope of  $L_\theta$ . In fact, the width of palm lines is usually larger than one pixel, and  $L_\theta$  is further extended to represent the set of points that make up a line with angle  $\theta$  and line width  $d$ . Figure 4 shows six  $16 \times 16$  MFRAT templates used in RLOC feature extraction. Since the palm lines are negative, the orientation of center point  $I(i_0, j_0)$  is determined using the winner-takes-all rule

$$w_{(i_0, j_0)} = \arg \min_k (MFRAT_I(i_0, j_0, \theta_k)), k = 0, 1, \dots, 5, \quad (7)$$

where  $w_{(i_0, j_0)}$  is the winner index.

In the matching stage, the winner index 0~5 can be encoded into corresponding 3-bit bitwise representation 000, 001, 010, 011, 100, 101. Given two RLOC codes  $\mathbf{P}$  and  $\mathbf{Q}$ , the distance

$$d_{RLOC} = \frac{\sum_{x=1}^N \sum_{y=1}^N (P_M(x, y) \cap Q_M(x, y)) n_{\{\cup_{i \in \{1, 2, 3\}} (P_i(x, y) \otimes Q_i(x, y))\}}}{\sum_{x=1}^N \sum_{y=1}^N (P_M(x, y) \cap Q_M(x, y))} \quad (8)$$

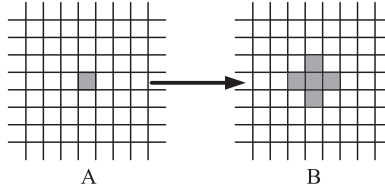


Fig. 5. The pixel-to-area comparison scheme [Jia et al. 2008].

is then used to enforce fast matching, where  $P_i$  and  $Q_i$  are the  $i$ th bit planes ( $i = 1, 2, 3$ ) of  $\mathbf{P}$  and  $\mathbf{Q}$ ,  $P_M$  and  $Q_M$  are the masks of  $\mathbf{P}$  and  $\mathbf{Q}$ ,  $\otimes$  is a bitwise exclusive OR (XOR) operator,  $\cap$  is a bitwise AND operator, and  $\cup$  is a bitwise OR operator. To improve the fault toleration ability, RLOC adopts a pixel-to-area matching scheme, where each pixel in  $\mathbf{P}$  is compared with the neighborhood of the corresponding pixel in  $\mathbf{Q}$ , as shown in Figure 5.

Compared with competitive code and ordinal code, RLOC has a faster feature extraction speed because the implementation of MFRAT only uses a summation operation. Since RLOC adopts the pixel-to-area comparison scheme, the matching speed of RLOC would be much slower.

**4.3.4 DoG Code.** The DoG code uses the vertical and horizontal derivatives of Gaussian filters for filtering the palmprint images, and then encodes the filtering responses into bitwise codes [Wu et al. 2006]. The method first resizes the original palmprint image to  $32 \times 32$ , then uses the horizontal and vertical derivatives of 2D Gaussian filters

$$G_x(x, y, \sigma) = \frac{-x}{2\pi\sigma^4} \exp\left(-\frac{x^2 + y^2}{2\sigma^2}\right), \quad (9)$$

$$G_y(x, y, \sigma) = \frac{-y}{2\pi\sigma^4} \exp\left(-\frac{x^2 + y^2}{2\sigma^2}\right), \quad (10)$$

to convolve with the  $32 \times 32$  palmprint image, and obtains the filtering responses  $I_x$  and  $I_y$ .

The palmprint image is then encoded into two  $32 \times 32$  bitwise matrices according to the sign of the filtering responses,  $C_x, C_y$ .  $C = (C_x, C_y)$  is the DoG code. In the matching stage, the DoG code adopts the Hamming distance used by PalmCode [Wu et al. 2006].

**4.3.5 Wide Line Detector.** Given a palmprint image  $I(x, y)$ , wide line detector first measures the similarity of brightness within a circular mask and the brightness at the center of the mask in a weighted mask having similar brightness (WMSB) [Liu et al. 2007]

$$s(x, y, x_0, y_0, t) = \operatorname{sech}\left(\frac{I(x, y) - I(x_0, y_0)}{t}\right)^5, \quad (11)$$

where  $\operatorname{sech}(x) = 2/(e^x + e^{-x})$ ,  $(x_0, y_0)$  denotes the center, and  $(x, y)$  denotes the coordinate of any other pixel within the mask, and  $t$  is the brightness contrast threshold. Taking into account the effect of the relative location to the center, a square weighting function  $w(x, y, x_0, y_0, r)$  is introduced to weigh the circular mask with constant weighting or a Gaussian profile. The weighting comparison is then determined by

$$c(x, y, x_0, y_0, t) = w(x, y, x_0, y_0, t) \times s(x, y, x_0, y_0, t). \quad (12)$$

The WMSB mass of the center  $(x_0, y_0)$  is obtained by

$$m(x_0, y_0) = \sum_{(x-x_0)^2+(y-y_0)^2 \leq r^2} c(x, y, x_0, y_0). \quad (13)$$

Finally, the line response  $L$  is defined as the inverse WMSB mass

$$L(x_0, y_0) = \begin{cases} g - m(x_0, y_0), & \text{if } m(x_0, y_0) < g \\ 0, & \text{else} \end{cases}, \quad (14)$$

where  $g$  is the geometric threshold with  $g = \pi r^2/2$ . In wide line detector, the contrast threshold  $t$  is defined as the standard deviation of the image  $I$ , and the radius of the circular mask is determined with the constraint

$$r \geq 2.5w, \quad (15)$$

where  $2w$  is the width of the estimated palm line.

During the matching stage, the method adopts the matching score [Liu and Zhang 2005] defined by

$$s(P, Q) = \frac{2}{M_P + M_Q} \times \sum_{i=1}^{M_Q} P(x_i, y_i), \quad (16)$$

where  $P$  and  $Q$  are two line images,  $M_P$  and  $M_Q$  are the number of line points in  $P$  and  $Q$ ,  $(x_i, y_i)$  ( $i = 1, \dots, M_Q$ ) is the coordinate of line points in palm-line image  $Q$ , and  $P(x_i, y_i)$  denotes whether point  $(x_i, y_i)$  is a line pixel.

**4.3.6 Fisherpalms.** Let  $\mathbf{X} = \{\mathbf{x}_1^{(1)}, \mathbf{x}_2^{(1)}, \dots, \mathbf{x}_{N_1}^{(1)}, \dots, \mathbf{x}_j^{(i)}, \dots, \mathbf{x}_{N_c}^{(C)}\}$  be a training set with  $N_i$  palmprint image vectors for class  $i$ . The number of the class is  $C$ , and  $\mathbf{x}_j^{(i)}$  denotes the  $j$ th image of class  $i$ . The total covariance matrix  $\mathbf{S}_t$  is defined as

$$\mathbf{S}_t = \frac{1}{N} \sum_{i=1}^C \sum_{j=1}^{N_i} (\mathbf{x}_j^{(i)} - \bar{\mathbf{x}})(\mathbf{x}_j^{(i)} - \bar{\mathbf{x}})^T, \quad (17)$$

where  $\bar{\mathbf{x}}$  is the mean vector of all training images, and  $N$  is the total number of training images. The PCA projector  $\mathbf{T}_{pca} = [\varphi_1, \varphi_2, \dots, \varphi_{d_{PCA}}]$  can be obtained by calculating the eigenvectors of the total scatter matrix  $\mathbf{S}_t$ , and  $d_{PCA}$  is the number of eigenvectors to guarantee the nonsingularity of the within-class scatter matrix,  $d_{PCA} = N - C$ .

The between-class scatter matrix  $\mathbf{S}_b$  and the within-class scatter matrix  $\mathbf{S}_w$  are defined as

$$\mathbf{S}_b = \frac{1}{N} \sum_{i=1}^C N_i (\bar{\mathbf{x}}^{(i)} - \bar{\mathbf{x}})(\bar{\mathbf{x}}^{(i)} - \bar{\mathbf{x}})^T, \quad (18)$$

$$\mathbf{S}_w = \frac{1}{N} \sum_{i=1}^C \sum_{j=1}^{N_i} (\mathbf{x}_j^{(i)} - \bar{\mathbf{x}}^{(i)})(\mathbf{x}_j^{(i)} - \bar{\mathbf{x}}^{(i)})^T, \quad (19)$$

where  $\bar{\mathbf{x}}^{(i)}$  is the mean vector of class  $i$ . With the PCA projector  $\mathbf{T}_{pca}$ , we map  $\mathbf{S}_b$  and  $\mathbf{S}_w$  to the corresponding transformed matrices,

$$\tilde{\mathbf{S}}_b = \mathbf{T}_{pca}^T \mathbf{S}_b \mathbf{T}_{pca}, \quad (20)$$

and

$$\tilde{\mathbf{S}}_w = \mathbf{T}_{pca}^T \mathbf{S}_w \mathbf{T}_{pca}. \quad (21)$$

The standard Fisher's linear discriminant is used to obtain the optimal discriminant vectors

$$J_F(\mathbf{u}) = \frac{\mathbf{u}^T \tilde{\mathbf{S}}_b \mathbf{u}}{\mathbf{u}^T \tilde{\mathbf{S}}_w \mathbf{u}} = \frac{\mathbf{u}^T \mathbf{T}_{pca}^T \mathbf{S}_b \mathbf{T}_{pca} \mathbf{u}}{\mathbf{u}^T \mathbf{T}_{pca}^T \mathbf{S}_w \mathbf{T}_{pca} \mathbf{u}}. \quad (22)$$

Let  $\mathbf{W}_{FLD} = [\mathbf{u}_1, \mathbf{u}_2, \dots, \mathbf{u}_{d_{LDA}}]$ , where  $d_{LDA}$  is the number of discriminant vectors. The discriminant vectors in the original space are obtained by

$$\mathbf{W}_{opt} = \mathbf{T}_{PCA} \mathbf{W}_{fld} = [\mathbf{w}_1, \mathbf{w}_2, \dots, \mathbf{w}_{d_{LDA}}], \quad (23)$$

where each column of  $\mathbf{W}_{opt}$  is called a *Fisherpalm* [Wu et al. 2003]. In Fisherpalms, each sample is first transformed to the Fisherpalm space,

$$\mathbf{z}^s = \mathbf{W}_{opt}^T \mathbf{x}, \quad (24)$$

and the nearest neighbor classifier is used for palmprint matching.

**4.3.7 DCT+LDA.** Let  $\mathbf{X} = \{\mathbf{X}_1^{(1)}, \mathbf{X}_2^{(1)}, \dots, \mathbf{X}_{N_1}^{(1)}, \dots, \mathbf{X}_j^{(i)}, \dots, \mathbf{X}_{N_c}^{(C)}\}$  be a training set with  $N_i$  palmprint images for class  $i$ . The number of the class is  $C$ , and  $\mathbf{X}_j^{(i)}$  denotes the  $j$ th  $M \times N$  ( $M \geq N$ ) image of class  $i$ . DCT is performed on each image  $\mathbf{X}_j^{(i)}$  to obtain the transformed image  $\mathbf{Y}_j^{(i)}$ . Jing and Zhang [2004] divided the transformed image  $\mathbf{Y}_j^{(i)}$  into  $M$  frequency bands, where the  $k$ th frequency band is a half square ring  $\mathbf{Y}_{j,k}^{(i)}$ .

After defining the within- and between-class scatter matrices  $\mathbf{S}_w$  and  $\mathbf{S}_b$  for each frequency band, the reparability of the frequency band is evaluated using the following criterion

$$\mathcal{J}(Y_k) = \frac{tr(\mathbf{S}_b)}{tr(\mathbf{S}_w)}, \quad (25)$$

where  $tr(\cdot)$  denotes the trace of the matrix. For each image  $\mathbf{X}$ , we choose the frequency bands where  $\mathcal{J}(Y_k)$  is higher than a threshold  $T$ , and obtain a one-dimensional sample vector  $\mathbf{z}$ . Then, Fisherpalms are performed on the sample vectors and nearest neighbor classifier is used for palmprint matching. The procedure of the feature extraction and representation of DCT+LDA is shown in Figure 6 [Jing and Zhang 2004].

## 5. EXPERIMENTAL RESULTS

A palmprint recognition algorithm usually involves several parameters that should be tuned to meet the real application environment. To determine the parameter values of each algorithm, we construct an isolated training set of 2400 images captured from 100 individuals, of 200 palms. Not all the training samples are used in our verification and identification experiments. The training images are captured using the same device that was adopted to build the HKPU palmprint database. The samples of each individual were also collected in two sessions, where the average interval between the first and the second sessions was around one month. During each session, we captured six palmprint images each of the left and the right palms.

For each algorithm, we tested a wide range of parameters to investigate its best performance. The parameters that produce the minimum EER value on the training set are regarded as the optimal parameters. All the experimental results listed in the following are obtained using the HKPU palmprint database based on the optimal parameters of each algorithm.

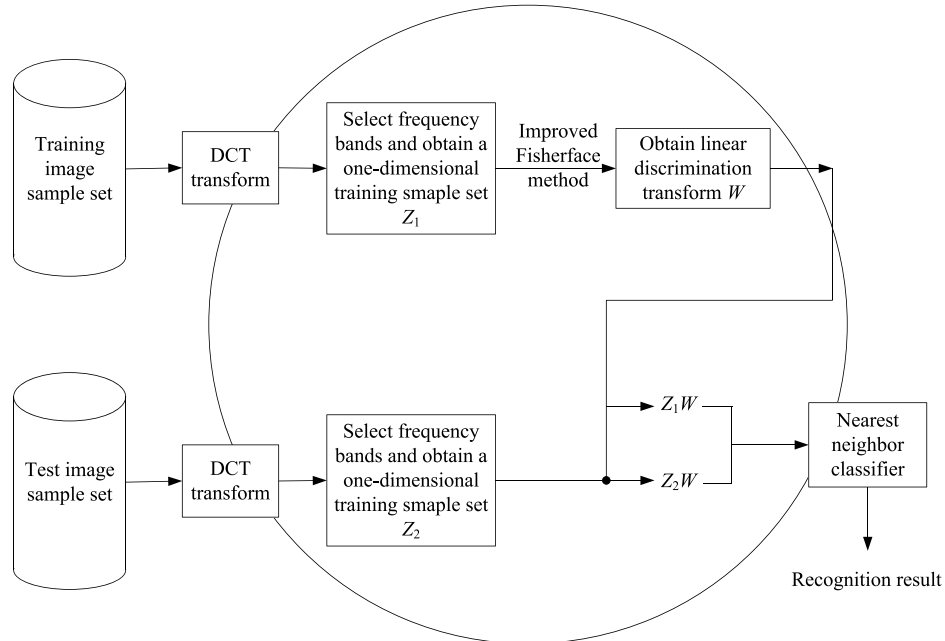


Fig. 6. Schematic diagram of DCT+LDA [Jing and Zhang 2004].

### 5.1 Verification Performance

Since the HKPU database contains two sessions, three sets of experiments are carried out to evaluate the verification performance of each algorithm.

- (1) *Set 1.* Verification performance of each algorithm obtained by matching palmprints from the first session.
- (2) *Set 2.* Verification performance of each algorithm obtained by matching palmprints from the second session.
- (3) *Set 3.* Verification performance of each algorithm obtained by matching palmprints from different sessions.

The first and the second sets of experiments are designed to evaluate the performance of each method in comparing palmprints of the same session, and thus can show the performance of within-session matching over a period of the time. The third set of experiments is designed to evaluate the robustness of each method in comparing palmprint from different sessions. Since in real applications, the template image and the test image are usually captured from different time periods, the performance obtained by the third set of experiments is more meaningful in an algorithm performance comparison.

The EER and  $GAR_{-3}$  values of all the algorithms in the three sets of verification experiments are listed in Table VII. In the first set of experiments, competitive code and ordinal code are superior in terms of EER and  $GAR_{-3}$  values. In the second set of experiments, competitive code and RLOC outperform the other recognition methods in terms of both EER and  $GAR_{-3}$  values. In the third set of experiments, competitive code achieves the lowest EER and the highest  $GAR_{-3}$ . Figure 7 shows the ROC curves of the algorithms for the three sets of experiments. From Table VII and Figure 7, it is obvious to observe the following.

Table VII. Results of Three Sets of Verification Experiments

		<i>CompCode</i>	<i>OrdiCode</i>	<i>DoG Code</i>	<i>RLOC</i>	<i>WLD</i>	<i>Fisherpalms</i>	<i>DCT + LDA</i>
Set 1	EER(%)	0.006	0.005	0.023	0.022	0.220	3.510	2.716
	$GAR_{-3}(\%)$	99.98	99.98	99.91	99.95	99.40	81.48	90.21
Set 2	EER(%)	0.011	0.051	0.061	0.027	0.086	3.112	2.372
	$GAR_{-3}(\%)$	99.95	99.83	99.77	99.91	99.53	76.05	84.23
Set 3	EER(%)	<b>0.058</b>	0.138	0.216	0.131	0.511	9.137	7.204
	$GAR_{-3}(\%)$	<b>99.65</b>	97.93	96.23	98.93	94.64	22.43	31.50

- (1) For each algorithm, the error rates obtained on Set 3 are much lower than those on Set 1 and Set 2. Since practical applications usually involve matching samples acquired at different time-stages, we recommend using the verification accuracy on Set 3 to evaluate palmprint recognition methods.
- (2) Compared with local feature-based methods, holistic methods, i.e., Fisherpalms and DCT+LDA, may perform well on Set 1 and Set 2, but their accuracy would decrease dramatically on Set 3.
- (3) Competitive code is consistently better than the other methods in terms of verification accuracy, and is more effective for matching palmprints from different sessions.

To discuss the performance difference between palmprint recognition algorithms, we could use several recently developed statistical methods to construct the confidence intervals for error rates [Guyon et al. 1998; Dass et al. 2006]. Although the multiple samples of the biometric entity may be not statistically independent, for simplicity, we still use the method in Guyon et al. [1998] to evaluate the performance improvement of the palmprint recognition method. Following Guyon et al. [1998], we discuss the statistical significance in the performance difference between different algorithms. Let  $\alpha$  be the confidence interval, and  $e$  and  $\hat{e}$  be the error rate of a classifier  $C$  and the estimated error rate using a test set with finite samples. In Guyon et al. [1998], at the  $\alpha$ -confidence level, if the number of trials  $N$  is larger than a threshold, the true error rate would not exceed the error rate by an amount larger than  $\varepsilon(N, \alpha) = \beta e$ . Assuming that recognition errors are Bernoulli trials, given a typical value of  $\alpha = 0.05$  and a typical value of  $\beta = 0.2$ , Guyon et al. proposed a simple equation to determine the number of trials  $N \approx 100/e$  to achieve  $(1 - \alpha)$  confidence in the error rate estimation.

Because the performance indicators obtained in Set 3 are more valuable for reflecting the verification performance of each algorithm, we discuss the statistical significance of the performance difference of Set 3. In this set of experiments, the number of genuine and imposter comparisons are 38,924 and 14,984,283, respectively. Thus the statistical significance could be guaranteed with an empirical error rate up to  $0.66 \times 10^{-3}\%$ . From Table VII, both the EER value and the  $(1-GAR_{-3})$  value of CompCode are 20% lower than those of the other methods, and are higher than  $0.66 \times 10^{-3}\%$ . Thus one can say that CompCode achieves the highest verification performance among these methods.

The verification experimental results show that, local feature-based methods generally achieve lower EER and higher  $GAR_{-3}$  values than the two holistic methods. This may be explained as follows. First, Fisherpalms and DCT+LDA require estimating scatter matrices, and the limited training set size would cause the poor estimation and overfitting of the scatter matrices; second, the inter- and intra-subject variations of palmprint images are complicated and nonlinear, and thus it is difficult to learn an appropriate holistic model from only a limited training set and to generalize the model to any palmprint population.

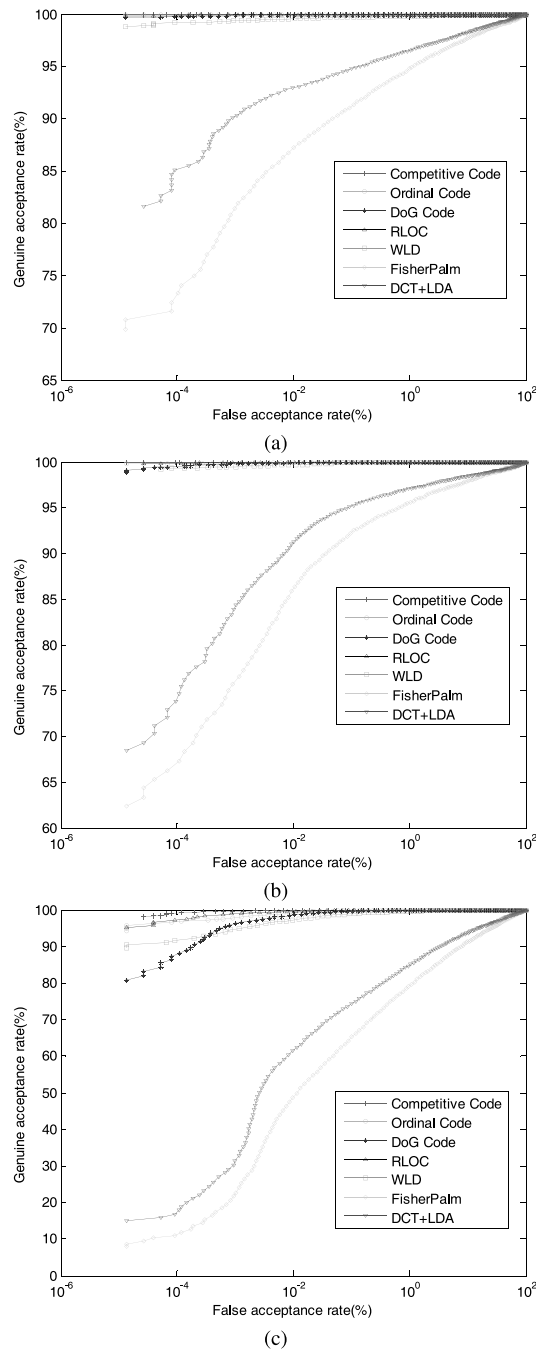


Fig. 7. The ROC curves of all the algorithms in the three sets of verification experiments—(a) Set 1, (b) Set 2, and (c) Set 3.

Table VIII. Results of Identification Experiments

		<i>CompCode</i>	<i>OrdiCode</i>	<i>DoG Code</i>	<i>RLOC</i>	<i>WLD</i>	<i>Fisherpalms</i>	<i>DCT + LDA</i>
EER (std,%)	TestSet 1	0 (0)	0 (0)	0.009 (0.016)	0.004 (0.011)	0.096 (0.051)	3.711 (0.166)	2.210 (0.214)
	TestSet 2	0.133 (0.026)	0.962 (0.136)	0.940 (0.112)	0.313 (0.059)	1.373 (0.143)	20.007 (0.498)	15.375 (0.384)
GAR <sub>2</sub> (std,%)	TestSet 1	100 (0)	100 (0)	99.99 (0.02)	99.99 (0.01)	99.87 (0.07)	88.78 (0.61)	93.95 (0.41)
	TestSet 2	99.59 (0.17)	96.57 (1.31)	93.10 (2.79)	98.97 (0.29)	96.00 (0.57)	12.64 (3.33)	25.74 (2.59)
IR (std,%)	TestSet 1	100 (0)	100 (0)	100 (0)	100 (0)	99.97 (0.0002)	99.54 (0.0013)	99.77 (0.0009)
	TestSet 2	99.99 (0.0001)	99.98 (0.0003)	99.96 (0.0003)	99.98 (0.0003)	99.82 (0.001)	91.40 (0.0007)	94.99 (0.004)

Local feature-based methods usually utilize prior knowledge of the palmprint to derive effective and compact representation of local features, and thus would be more robust for matching between different sessions than holistic methods [Kong 2007]. Among the five local feature-based methods, *CompCode* and *RLOC* encode the orientation information, *OrdiCode* encodes the ordinal information, *DoGCode* encodes the sign of the filter responses, and *WLD* encodes the position information of palm lines. The superiority of *CompCode* over the other methods might be attributed to the fact that, for palmprint recognition, appropriate representation of orientation information would be more effective and robust than ordinal, filter response sign, and palm line location information. In future research, it would be an interesting direction to develop effective and compact representation of local features. Some recent developments also verify the effectiveness of local feature representation [Chen et al. 2010; Guo et al. 2009; Yue et al. 2009].

As shown in Table VII, although the two holistic methods do not outperform local feature-based methods, there is still the possibility of improving the palmprint verification performance by combining both holistic and local feature-based methods. In Section 6, we will discuss this problem by investigating the error correlation and fusion performance of the holistic and local feature-based methods.

Finally, we discuss the verification accuracy of palmprint traits with other commonly used biometric modalities. Jain et al. [2007] summarized the state-of-the-art false accept and false reject rates associated with fingerprint, face, voice, and iris modalities. Compared with these biometric modalities, palmprint can achieve comparable or better verification accuracy. It should be noted that, the accuracy of biometric systems depends on a number of noise factors and test conditions: the sensor, subject disposition, and habituation. Thus, more comprehensive independent three-party tests should be conducted to obtain an objective evaluation on palmprint traits and the other biometric modalities.

## 5.2 Identification Performance

Following the identification evaluation protocol described in Section 4.2, we evaluate the identification performance of different algorithms. Table VIII lists the EER, GAR<sub>2</sub>, and identification rate (IR) of each algorithm on TestSet 1 and TestSet 2. Figure 8 shows the ROC curves of different algorithms using TestSet 1 and TestSet 2. Experimental results show that, since the samples for TestSet 1 are captured from the same session as the samples from the template set, most methods could achieve high identification rate, low EER, and high GAR<sub>2</sub> values. For TestSet 2, competitive code outperforms the other methods in terms of identification rate, EER, and

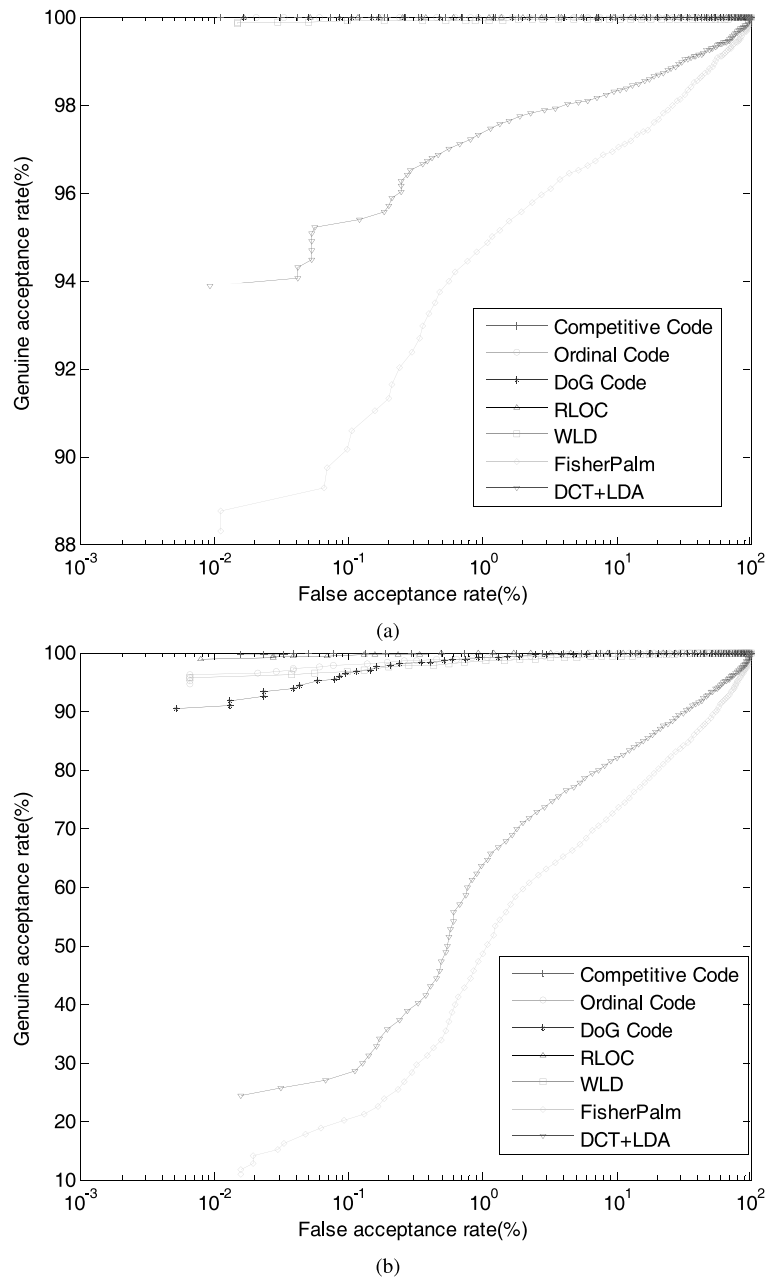


Fig. 8. The ROC curves of all the algorithms in identification experiments on (a) TestSet 1, and (b) TestSet 2.

GAR<sub>2</sub> values. The results are consistent with the results in Section 5.1, which indicate that competitive code is more robust for identifying palmprints from different sessions.

Table IX. Template Size (bytes) of All the Algorithms

CompCode	OrdiCode	DoG Code	RLOC	WLD	Fisherpalms	DCT+LDA
384	384	256	1024	512	1592	1448

Note: RLOC can also be stored in 384 bytes, but for fast matching, we prefer to store the feature in 1024 bytes.

Table X. Computational Time (ms) of All the Algorithms

	CompCode	OrdiCode	DoG Code	RLOC	WLD	Fisherpalms	DCT+LDA
<i>Feature extraction</i>	70	58	9.6	2.2	94	350	297
<i>Matching</i>	0.04	0.04	0.03	0.85	0.42	0.001	0.001

Experimental environment: Windows XP Professional, Pentium 4 2.66GHz, 512M RAM, VC 6.0.

### 5.3 Memory and Computational Requirements

Tables IX and X summarize the template size and computational time required by each algorithm. In general, the template sizes of all the local feature-based algorithms are below 1k bytes, which makes them very suitable for typical smart card applications. The relatively small template size of the DoG code is due to a smaller number of filters used, while for the competitive and ordinal codes, each sample point is encoded into 3-bit code by six filters. Furthermore, the computation time for feature extraction and matching is far below 1 second, which suits them for online personal identification. Note that the matching speed for the competitive, ordinal and DoG codes is sufficiently fast. As for RLOC, its shortest feature extraction time is mainly due to the integer template it adopted, while the pixel-to-area matching contributes to its longest matching time.

Compared with the local feature-based algorithms, the two holistic methods use real numbers to represent the feature vector, and thus have relatively larger template sizes. Besides, as shown in Table X, since of their small feature dimensions (less than 200), the two holistic methods have much faster matching speeds than the local feature-based algorithms. The fast matching speed characteristic of holistic methods could be used for efficient hierarchical palmprint identification, where the holistic methods are first used for coarse matching to identify most imposters before the final fine matching.

## 6. CORRELATION ANALYSIS AND SCORE LEVEL FUSION

Previous research suggests that the fusion of different algorithms could lead to improved accuracy. In this section, following Cappelli et al. [2006], we first investigate the error correlation of difficulty values for different algorithms. Based on these correlation values, we then study the fusion performance of different palmprint recognition algorithms by using several score-level fusion methods that are frequently used in biometric research.

### 6.1 Analysis of Error Correlation

In Cappelli et al. [2006], error correlation is used to measure the correlation of the difficulty values of two algorithms. Given an algorithm  $A$ , we can calculate the matching score  $s$  of two palmprint images,  $I_1$  and  $I_2$ . If this matching is an impostor comparison, we use the false rejection rate of the algorithm  $A$  with threshold  $s$  to denote the genuine difficulty value  $DV_G(A, I_1, I_2)$  of palmprint pair  $I_1$  and  $I_2$ . Similarly, If this

Table XI. Genuine Matching: Correlation Coefficient of the Corresponding Difficulty Values for all the Algorithms

	<i>CompCode</i>	<i>OrdiCode</i>	<i>DoG Code</i>	<i>RLOC</i>	<i>WLD</i>	<i>Fisherpalms</i>	<i>DCT + LDA</i>
<i>CompCode</i>	1.0000	-	-	-	-	-	-
<i>OrdiCode</i>	0.9189	1.0000	-	-	-	-	-
<i>DoG Code</i>	0.8598	0.8645	1.0000	-	-	-	-
<i>RLOC</i>	0.7671	0.7806	0.8330	1.0000	-	-	-
<i>WLD</i>	0.7493	0.7759	0.7910	0.8128	1.0000	-	-
<i>Fisherpalms</i>	0.4916	0.4789	0.6329	0.6537	0.6472	1.0000	-
<i>DCT + LDA</i>	0.4810	0.4879	0.6256	0.6335	0.6307	0.9569	1.0000

Table XII. Imposter Matching: Correlation Coefficient of the Corresponding Difficulty Values for all the Algorithms

	<i>CompCode</i>	<i>OrdiCode</i>	<i>DoG Code</i>	<i>RLOC</i>	<i>WLD</i>	<i>Fisherpalms</i>	<i>DCT + LDA</i>
<i>CompCode</i>	1.0000	-	-	-	-	-	-
<i>OrdiCode</i>	0.6798	1.0000	-	-	-	-	-
<i>DoG Code</i>	0.5945	0.6549	1.0000	-	-	-	-
<i>RLOC</i>	0.4617	0.4614	0.4364	1.0000	-	-	-
<i>WLD</i>	0.2656	0.3424	0.2345	0.4655	1.0000	-	-
<i>Fisherpalms</i>	0.1761	0.2071	0.2508	0.3359	0.1753	1.0000	-
<i>DCT + LDA</i>	0.2954	0.3200	0.3802	0.4729	0.2423	0.8763	1.0000

matching is an imposter comparison, we use the false accept rate of the algorithm  $A$  with the threshold  $s$  to denote the imposter difficulty value  $DV_I(A, I_1, I_2)$  of palmprint pair  $I_1$  and  $I_2$ . Using difficulty values, we further define the error correlation of the genuine matching of two algorithms as the correlation coefficient of their genuine difficulty values. Analogously, we define the error correlation of the imposter matching.

Tables XI and XII report the correlation coefficients of the algorithms. It can be observed that there are evident differences in correlation coefficients between genuine and imposter matching. The correlation of imposter matching is much lower than that of genuine matching. The reason for this result is that the difficulty of genuine matching is mainly caused by several noise factors of samples (such as illumination variance, distortion, etc.), whereas that of imposter matching is due to the different feature extraction and matching methods that they adopt.

Another observation is the strong correlation on genuine matching of algorithms, especially for *CompCode* and *OrdiCode*, which implies that the algorithms tend to make similar errors. Generally, the correlation between holistic methods and local feature-based methods is relatively small, while strong correlation is usually observed within the two holistic methods and within the five local feature-based methods.

## 6.2 Score Level Fusion

Score normalization usually is necessary for many score level fusion methods. In our fusion evaluation, we use four well known normalization methods and four score-level fusion methods. For score normalization, we tested the four score normalization rules presented in Snelick et al. [2005] and Jain et al. [2005].

- (1) *Min-Max (MM) normalization*. Given the minimum ( $\min(S)$ ) and the maximum ( $\max(S)$ ) of the matching scores, this rule normalized the raw score  $s$  to the  $[0,1]$  range,

$$n_{MM} = \frac{s - \min(S)}{\max(S) - \min(S)}. \quad (26)$$

- (2) *Z-score (ZS) normalization*. Given the mean ( $mean(S)$ ) and the standard deviation ( $std(S)$ ) of the matching scores, this rule normalized the raw score  $s$  to follow a zero-mean distribution with standard deviation of 1,

$$n_{ZS} = \frac{s - mean(S)}{std(S)}. \quad (27)$$

- (3) *Tanh (TH) normalization*. Given the mean ( $mean(S)$ ) and the standard deviation ( $std(S)$ ) of the matching scores, according to robust statistics, this rule normalized the raw score  $s$  to the  $[0,1]$  range,

$$n_{TH} = \frac{1}{2} \left[ \tanh \left( \frac{0.01(s - mean(S))}{std(S)} \right) + 1 \right]. \quad (28)$$

- (4) *Adaptive Quadric-Line-Quadric (QLQ) normalization*. Given the minimum ( $min(S)$ ) and the maximum ( $max(S)$ ) of the matching scores, this rule further maps the MM normalization score using a piecewise function,

$$n_{TH} = \begin{cases} \frac{1}{c - \frac{w}{2}} n_{MM}^2, & n_{MM} \leq c - \frac{w}{2} \\ n_{MM} & c - \frac{w}{2} \leq n_{MM} \leq c + \frac{w}{2} \\ (c + \frac{w}{2}) + \sqrt{(1 - c - \frac{w}{2})(n_{MM} - c - \frac{w}{2})} & \text{otherwise} \end{cases}, \quad (29)$$

where the center  $c$  and the width  $w$  are two parameters of the QLQ normalization, that should be determined using a training set.

In score level fusion, we evaluate the fusion performance by using the four score level fusion methods, simple sum (SS), matcher weighting (MW), support vector machine (SVM), and likelihood ratio (LR) - based score fusion [Ben-Yacoub et al. 1999; Nandakumar et al. 2008; Snelick et al. 2005]. The reason to choose SS and MW is that they generally outperform several other simple fusion methods in Snelick et al. [2005]. The reason to choose SVM is that it is a state-of-the-art classifier and thus is representative in classifier-based score fusion. The reason to choose LR is that it is a recently developed high performance score fusion method. Given  $M$  matchers, we let  $n_m$  denote the normalized matching score of the matcher  $m$  ( $m = 1, 2, \dots, M$ ), the fusion method aims to derive a fusion score with a fusion function  $n_F = f(n_1, \dots, n_M)$ .

- (1) *Simple Sum (SS)*. This method calculates the SS fusion score using  $n_F = \sum_{m=1}^M n_m$ .  
 (2) *Matcher Weighting (MW)*. According to its EER,  $e_m$ , each matcher  $m$  is assigned to a weight  $w_m$ ,

$$w_m = \frac{1/e_m}{\sum_{k=1}^M 1/e_k}, \quad (30)$$

and the MW fusion score is then derived as  $n_F = \sum_{m=1}^M w_m n_m$ .

- (3) *Support Vector Machine (SVM)*. This method uses a feature vector to represent the scores from multiple matchers, and then trains an SVM classifier for personal identification. The OSU SVM toolbox<sup>4</sup> is used for SVM training and classification. We considered two types of kernels: Gaussian RBF and polynomial. Hereafter we call them RBF-SVM and Poly-SVM, respectively. The hyper-parameter  $C$  is chosen from  $\{0.01, 0.1, 1, 10, 100, 1000, 10000\}$ . For RBF-SVM, the hyper-parameter  $\sigma$  is chosen from  $\{0.01, 0.1, 1, 10, 100\}$ , and for Poly-SVM the hyper-parameter  $d$  is

<sup>4</sup>[http://www.ece.osu.edu/~maj/osu\\_svm/](http://www.ece.osu.edu/~maj/osu_svm/)

Table XIII. The EER (%) Values of Different Fusion Methods by Combining CompCode+OrdiCode+RLOC

	<i>Sum</i>	<i>MW</i>	<i>LR</i>	<i>SVM</i>
<i>MM</i>	0.035	0.029	0.026	0.030
<i>ZS</i>	0.033	0.027	0.026	0.032
<i>TH</i>	0.033	0.027	0.027	0.028
<i>QLQ</i>	0.035	0.029	0.036	0.031
<i>CompCode</i>	0.036			

Table XIV. The GAR<sub>-3</sub> (%) Values of Different Fusion Methods by Combining CompCode+OrdiCode+RLOC

	<i>Sum</i>	<i>MW</i>	<i>LR</i>	<i>SVM</i>
<i>MM</i>	99.86	99.90	99.91	99.83
<i>ZS</i>	99.88	99.90	99.91	99.87
<i>TH</i>	99.88	99.90	99.91	99.90
<i>QLQ</i>	99.86	99.89	99.79	99.89
<i>CompCode</i>	99.81			

Table XV. The EER (%) Values of Different Fusion Methods by Combining CompCode+Fisherpalms

	<i>Sum</i>	<i>MW</i>	<i>LR</i>	<i>SVM</i>
<i>MM</i>	0.268	0.037	0.033	0.045
<i>ZS</i>	0.109	0.037	0.035	0.044
<i>TH</i>	0.109	0.037	0.034	0.044
<i>QLQ</i>	0.205	0.037	0.037	0.045
<i>CompCode</i>	0.036			

chosen from  $\{ 1, 2, 3, 4, 5 \}$ . In our experiments, we first use the 3-fold cross-validation test on the training set to determine the kernel type and the values of the hyper-parameters, and then use all the samples in the training set to train a SVM.

- (4) *Likelihood Ratio-based Fusion (LR)*. This method first utilizes a finite Gaussian mixture model for modeling the genuine and imposter score densities, and then adopts the likelihood ratio test to derive the fusion score [Nandakumar et al. 2008].

A training set and a test set are constructed for the training and evaluation of the fusion method. Following the evaluation protocol adopted in Nandakumar et al. [2008], in each experiment, half of the genuine and half of the imposter matching scores are randomly selected to construct a training set, and the remaining are used for testing. The training set is used to determine the parameters (e.g.,  $\min(S)$  and  $\max(S)$ ) and hyper-parameters (e.g.,  $C$  in SVM) of the normalization and fusion methods. To reduce the performance variations against training-test partitioning, we run the fusion method 10 times and use the average GAR<sub>-3</sub> values at a specific FAR value to denote the fusion performance.

In our fusion experiments, we test the fusion of three combinations of palmprint recognition algorithms, and evaluate the fusion performance according to the EER and GAR<sub>-3</sub> values. Using the normalization and fusion rules previously described, we first evaluate the fusion performance by combining three top-performance palmprint recognition methods, CompCode, OrdiCode, and RLOC. Tables XIII and XIV show the EER

Table XVI. The  $GAR_{-3}$  (%) Values of Different Fusion Methods by Combining CompCode+Fisherpalms

	<i>Sum</i>	<i>MW</i>	<i>LR</i>	<i>SVM</i>
<i>MM</i>	99.08	99.82	99.83	99.80
<i>ZS</i>	99.72	99.81	99.82	99.76
<i>TH</i>	99.72	99.81	99.83	99.85
<i>QLQ</i>	99.40	99.81	99.86	99.81
<i>CompCode</i>	99.81			

Table XVII. The EER (%) Values of Different Fusion Methods by Combining All the Seven Methods

	<i>Sum</i>	<i>MW</i>	<i>LR</i>	<i>SVM</i>
<i>MM</i>	0.081	0.032	0.028	0.042
<i>ZS</i>	0.062	0.031	0.030	0.035
<i>TH</i>	0.062	0.031	0.029	0.038
<i>QLQ</i>	0.079	0.032	0.035	0.045
<i>CompCode</i>	0.036			

Table XVIII. The  $GAR_{-3}$  (%) Values of Different Fusion Methods by Combining All the Seven Methods

	<i>Sum</i>	<i>MW</i>	<i>LR</i>	<i>SVM</i>
<i>MM</i>	99.62	99.89	99.90	99.74
<i>ZS</i>	99.77	99.90	99.90	99.68
<i>TH</i>	99.77	99.90	99.90	99.88
<i>QLQ</i>	99.65	99.89	99.85	99.84
<i>CompCode</i>	99.81			

and  $GAR_{-3}$  values of this combination form, respectively. The MM normalization + LR fusion method obtains an EER of 0.026% and a  $GAR_{-3}$  of 99.91%, which are better than the best individual method, CompCode.

We then evaluate the fusion performance by combining the two methods with less correlation, CompCode and Fisherpalms. Tables XV and XVI show the EER and  $GAR_{-3}$  values of this combination form, respectively. Even CompCode significantly outperforms Fisherpalms. By choosing appropriate normalization and fusion rules, the fusion method could achieve a lower EER value than CompCode. This result shows that holistic methods have a lower correlation with local feature-based methods, and could be used to further improve the palmprint recognition performance. Thus, it would be valuable to develop effective holistic methods that are less correlated with the state-of-the-art local feature-based methods, and to study powerful fusion methods for combining holistic and local feature-based palmprint recognition methods.

Finally, we evaluate the fusion performance by combining all seven palmprint recognition methods. Tables XVII and XVIII show the EER and  $GAR_{-3}$  values of this combination form, respectively. The MM normalization + LR fusion method obtains an EER of 0.028% and  $GAR_{-3}$  of 99.90%, which are better than those of any individual method. The experimental results indicate that, even where methods have high error correlation or great performance differences, fusion could be used to improve the recognition performance. Thus, it would be a promising direction to develop effective normalization/fusion approaches for future palmprint recognition.

From Tables XIII–XIV, it is observed that the MM normalization + LR fusion method outperforms the other normalization/fusion schemes in almost all fusion experiments. Following Snelick et al. [2005] and Nandakumar et al. [2008], we discuss the reasons for the good performance of MM+LR. First, the performance of the likelihood ratio test can be guaranteed by the Neyman-Pearson theorem. Second, the finite Gaussian mixture model [Jain and Figueiredo 2002] provides a flexible tool to estimate arbitrary densities of matching scores. Third, the superiority of the MM normalization has been demonstrated in Snelick et al. [2005]. Besides, the poor performance of QLQ+LR can be attributed to the fact that QLQ is a nonlinear method, which might make the distributions after QLQ normalization more difficult for Gaussian mixture modeling.

Following Guyon et al. [1998], we discuss the statistical significance in performance improvement of the fusion methods. Given a typical value of  $\alpha = 0.05$  and a typical value of  $\beta = 0.2$ , the number of trials to achieve  $(1 - \alpha)$  confidence in the error rate estimate can be calculated by  $N \approx 100/e$ . In our fusion experiments, the numbers of genuine and imposter comparisons are 37,034 and 14,984,404, respectively. Thus the statistical significance could be guaranteed with an empirical error rate up to  $0.67 \times 10^{-3}\%$  and an improvement of error rate up to 20%. In the experimental results listed in Table XIII, the highest performance improvement in EER is  $9.33 \times 10^{-3}\%$ , and the highest performance improvement in  $\text{GAR}_{-3}$  is  $9.65 \times 10^{-2}\%$ . Since both the EER and the  $(1 - \text{GAR}_{-3})$  values of the fusion method are 20% lower than those of CompCode, and all the empirical error rates are higher than  $0.67 \times 10^{-3}\%$ , we can regard score-level fusion as effective in improving the verification performance. Thus, it would be encouraging to develop more effective fusion methods for palmprint recognition.

## 7. DISCUSSION AND CONCLUSIONS

In this article, we first presented a survey of palmprint feature extraction and matching methods. Then we chose five state-of-the-art local feature-based and two holistic palmprint recognition algorithms, and carried out a comparative study to evaluate the performance and error correlation of these approaches. In our survey, we grouped current palmprint recognition methods into three categories: holistic-based, feature-based, and hybrid methods. In feature-based methods, coding-based methods, which usually encode the response of a bank of filters into bitwise codes, may be one class of the most efficient palmprint recognition algorithms in terms of recognition accuracy, computational, and memory requirements. Based on the categorization of palmprint recognition methods, we also compared the complexity of different algorithms, provided a brief survey of the palmprint recognition methods for partial recognition and different sensing techniques, and presented a review of the antispoofing methods.

In our comparative study, using the HKPU palmprint database (version 2), we compared five local feature-based algorithms (competitive code, ordinal code, robust linear orientation code, DoG code, and wide line detector) and two holistic methods (Fish-erpalm and DCT+LDA). Results of the experiments show that local feature-based methods outperform holistic methods in terms of several specified indicators, and it is encouraging to develop effective and compact representation of local features for effective palmprint recognition.

We further investigated the error correlation and score-level fusion of different algorithms. We had observed less correlation between holistic and local feature-based algorithms, and that score-level fusion is effective in improving the verification performance. Therefore, it would be valuable to develop effective holistic methods that are less correlated with the state-of-the-art local feature-based methods, and to study powerful fusion methods for combining palmprint recognition methods.

By far, current palmprint recognition methods have achieved satisfactory recognition accuracy, feature extraction, and matching speed with which build an online low resolution palmprint recognition system. However, robust palmprint recognition is still challenging. Several interesting directions, such as unconstrained acquisition, efficient palmprint representation and matching, palmprint quality evaluation, and recognition of palmprint images with poor quality, might be promising for future research.

In this article, we concentrate on the survey of low resolution palmprint recognition algorithms. With advances in sensor techniques and computational power, novel palmprint recognition methods have recently been investigated, for example, multispectral, latent, and 3D palmprint recognition. The experience with methods of low resolution palmprint recognition will be valuable for the future studies on these novel palmprint recognition technologies.

## REFERENCES

- AHONEN, T., HADID, A., AND PIETIKÄINEN, M. 2004. Face recognition with local binary patterns. In *Proceedings of the European Conference on Computer Vision*. 469–481.
- AHONEN, T., HADID, A., AND PIETIKÄINEN, M. 2006. Face description with local binary patterns: Application to face recognition. *IEEE Trans. Pattern Anal. Mach. Intell.* 28, 12, 2037–2041.
- ASHBAUGH, D. 1999. *Quantitative-Qualitative Friction Ridge Analysis: An Introduction to Basic and Advanced Ridgeology*. CRC Press.
- AYKUT, M. AND EKINCI, M. 2007. Palmprint recognition using wavelet based kernel pca. In *Proceedings of the IEEE 15th Signal Processing and Communications Applications*. 1–4.
- BEN-YACOB, S., ABDELJAOUED, Y., AND MAYORAZ, E. 1999. Fusion of face and speech data for person identity verification. *IEEE Trans. Neural Netw.* 10, 5, 1065–1074.
- CAPPELLI, R., MAIO, D., MALTONI, D., WAYMAN, J., AND JAIN, A. 2006. Performance evaluation of fingerprint verification systems. *IEEE Trans. Pattern Anal. Mach. Intell.* 28, 1 (Jan.), 3–18.
- CHEN, G. AND XIE, W. 2007. Pattern recognition with svm and dual-tree complex wavelets. *Image Vis. Comput.* 25, 6, 960–966.
- CHEN, J., MOON, Y., WONG, M., AND SU, G. 2010. Palmprint authentication using a symbolic representation of images. *Image Vis. Comput.* 28, 3, 343–351.
- CHEUNG, K., KONG, A., ZHANG, D., KAMEL, M., AND YOU, J. 2006. Does eigenpalm work? a system and evaluation perspective. In *Proceedings of the International Conference on Pattern Recognition*. 445–448.
- CNET. 2006. British police get palm print database. [http://news.cnet.com/British-police-get-palm-print-database/2100-11390\\_3-6053083.html](http://news.cnet.com/British-police-get-palm-print-database/2100-11390_3-6053083.html).
- CONNIE, T., JIN, A., ONG, M., AND LING, D. 2003. An automated palmprint recognition system. *Image Vis. Comput.* 23, 5, 501–515.
- CONNIE, T., TEOH, A., GOH, M., AND NGO, D. 2005. Palmhashing: A novel approach for cancelable biometrics. *Inf. Process. Lett.* 93, 1, 1–5.
- CUMMINS, H. AND MIDLO, M. 1961. *Finger Prints, Palms and Soles: An Introduction to Dermatoglyphics*. Dover.
- DAI, Q., BI, N., HUANG, D., ZHANG, D., AND LI, F. 2004. M-band wavelets applications to palmprint recognition based on texture features. In *Proceedings of the International Conference on Image Processing*. 893–896.
- DASS, S., ZHU, Y., AND JAIN, A. 2006. Validating a biometric authentication system: Sample size requirements. *IEEE Trans. Pattern Anal. Mach. Intell.* 28, 12, 1902–1913.
- DAUGMAN, J. 1993. High confidence visual recognition of persons by a test of statistical independence. *IEEE Trans. Pattern Anal. Mach. Intell.* 15, 11, 1148–1161.
- DODDINGTONA, G., PRZYBOCKI, M., MARTIN, A., AND REYNOLDS, D. 2000. The nist speaker recognition evaluation c overview, methodology, systems, results, perspective. *Speech Comm.* 31, 2-3, 225–254.
- DUTA, N., JAIN, A., AND MARDIA, K. 2002. Matching of palmprints. *Pattern Recog. Lett.* 23, 4), 477–485.
- EKINCI, M. AND AYKUT, M. 2007. Gabor-based kernel pca for palmprint recognition. *Electron. Lett.* 43, 20, 1077–1079.

- FIDLER, S., SKOČAJ, D., AND LEONARDIS, A. 2006. Combining reconstructive and discriminative subspace methods for robust classification and regression by subsampling. *IEEE Trans. Pattern Anal. Mach. Intell.* 28, 3, 337–350.
- GAO, Y. AND LEUNG, M. 2002. Face recognition using line edge map. *IEEE Trans. Pattern Anal. Mach. Intell.* 24, 6, 764–779.
- GARRIS, M., TABASSI, E., AND WILSON, C. 2006. Nist fingerprint evaluations and developments. *Proc. IEEE* 94, 11, 1915–1926.
- GUO, Z., ZHANG, D., ZHANG, L., AND ZUO, W. 2009. Palmprint verification using binary orientation co-occurrence vector. *Pattern Recogn. Lett.* 30, 13, 1219–1227.
- GUYON, I., MAKHOUL, J., SCHWARTZ, R., AND VAPNIK, V. 1998. What size test set gives good error rate estimates. *IEEE Trans. Pattern Anal. Mach. Intell.* 20, 1, 52–64.
- HAN, C. C. 2004. A hand-based personal authentication using a coarse-to-fine strategy. *Image Vis. Comput.* 22, 11 (Nov.), 909–918.
- HAN, C., CHENG, H., LIN, C., AND FAN, K. 2003. Personal authentication using palm-print features. *Pattern Recogn.* 36, 2, 371–381.
- HAN, Y., TAN, T., AND SUN, Z. 2007. Palmprint recognition based on directional features and graph matching. In *Proceedings of the International Conference on Biometrics*. 1164–1173.
- HAN, D., GUO, Z., AND ZHANG, D. 2008. Multispectral palmprint recognition using wavelet-based image fusion. In *Proceedings of the 9th International Conference on Signal Processing*. 2074–2077.
- HAO, Y., SUN, Z., AND TAN, T. 2007. Comparative studies on multispectral palm image fusion for biometrics. In *Proceedings of the Asia Conference on Computer Vision*. 12–21.
- HAO, Y., SUN, Z., TAN, T., AND REN, C. 2008. Multispectral palm image fusion for accurate contact-free palmprint recognition. In *Proceedings of the International Conference on Image Processing*. 281–284.
- HENNINGS, P., SAVVIDES, M., KUMAR, B., KAMEL, M., AND CAMPILHO, A. 2005. Verification of biometric palmprint patterns using optimal trade-off filter classifiers. In *Proceedings of the International Conference on Image Analysis and Recognition*. 1081–1088.
- HENNINGS-YEOMANS, P., KUMAR, B. V., AND SAVVIDES, M. 2007. Palmprint classification using multiple advanced correlation filters and palm-specific segmentation. *IEEE Trans. Inf. Forensics Secur.* 2, 3, 613–622.
- HU, D., FENG, G., AND ZHOU, Z. 2007. Two-dimensional locality preserving projection (2dlpp) with its application to palmprint recognition. *Pattern Recogn.* 40, 1, 339–342.
- HUANG, D., JIA, W., AND ZHANG, D. 2008. Palmprint verification based on principal lines. *Pattern Recogn.* 41, 4, 1316–1328.
- ITO, K., AOKI, T., NAKAJIMA, H., KOBAYASHI, K., AND HIGUCHI, T. 2006. A palmprint recognition algorithm using phase-based image matching. In *Proceedings of the International Conference on Image Processing*. 2669–2672.
- JAIN, A. AND FIGUEIREDO, M. 2002. Unsupervised learning of finite mixture models. *IEEE Trans. Pattern Anal. Mach. Intell.* 24, 3, 381–396.
- JAIN, A. AND DEMIRKUS, M. 2008. On latent palmprint matching. technical report. <http://biometrics.cse.msu.edu/Publications/Palmprints/OnLatentPalmprintMatchingJainDemirkus08.pdf>.
- JAIN, A. AND FENG, J. 2009. Latent palmprint matching. *IEEE Trans. Pattern Anal. Mach. Intell.* 31, 5, 1032–1047.
- JAIN, A. K., ROSS, A., AND PRABHAKAR, S. 2004. An introduction to biometric recognition. *IEEE Trans. Circuits Syst. Video Technol.* 14, 1, 4–20.
- JAIN, A., NANDAKUMAR, K., AND ROSS, A. 2005. Score normalization in multimodal biometric systems. *Pattern Recogn.* 38, 12, 2270–2285.
- JAIN, A., CHEN, Y., AND DEMIRKUS, M. 2007. Pores and ridges: High-resolution fingerprint matching using level 3 features. *IEEE Trans. Pattern Anal. Mach. Intell.* 29, 1, 15–27.
- JAIN, A., FLYNN, P., AND ROSS, A. 2007. *Handbook of Biometrics*. Springer.
- JIA, W., HUANG, D., AND ZHANG, D. 2008. Palmprint verification based on robust line orientation code. *Pattern Recogn.* 41, 5, 1504–1513.
- JING, X. AND ZHANG, D. 2004. A face and palmprint recognition approach based on discriminant dct feature extraction. *IEEE Trans. Syst. Man Cybern. Part B: Cybernetics* 34, 6, 2405–2415.
- JING, X. AND WONG, H. 2006. Biometrics recognition based on fused gaborface and gaborpalm with dcw-rbf feature classification. *Electron. Lett.* 42, 21, 1205–1206.

- JING, X., TANG, Y., AND ZHANG, D. 2005. A fourier-lda approach for image recognition. *Pattern Recog.* 38, 3, 453–457.
- JING, X., YAO, Y., ZHANG, D., YANG, J., AND LI, M. 2007. Face and palmprint pixel level fusion and kernel dc-v-rbf classifier for small sample biometric recognition. *Pattern Recog.* 27, 11, 3209–3224.
- KITTLER, J., HATEF, M., DUIN, R., AND MATAS, J. 1998. On combining classifiers. *IEEE Trans. Pattern Anal. Mach. Intell.* 20, 3, 226–239.
- KONG, A. 2007. Palmprint identification based on generalization of iriscodes. Ph.D. thesis, University of Waterloo, Canada.
- KONG, A. AND ZHANG, D. 2004. Competitive coding scheme for palmprint verification. In *Proceedings of the 17th International Conference on Pattern Recognition*. 520–523.
- KONG, W., ZHANG, D., AND LI, W. 2003. Palmprint feature extraction using 2-d gabor filters. *Pattern Recog.* 36, 10, 2339–2347.
- KONG, A., ZHANG, D., AND KAMEL, M. 2006a. Palmprint identification using feature-level fusion. *Pattern Recog.* 39, 3, 478–487.
- KONG, A., ZHANG, D., AND KAMEL, M. 2006b. A study of brute-force break-ins of a palmprint verification system. *IEEE Trans. Syst. Man Cybern. Part B* 36, 5, 1201–1205.
- KONG, A., CHEUNG, K., ZHANG, D., KAMEL, M., AND YOU, J. 2006. An analysis of bihashing and its variants. *Pattern Recog.* 39, 7, 1359–1368.
- KONG, A., ZHANG, D., AND KAMEL, M. 2008. Three measure for secure palmprint identification. *Pattern Recog.* 41, 4, 1329–1337.
- KONG, J., LU, Y., WANG, S., QI, M., AND LI, H. 2008. A two stage neural network-based personal identification systems using handprint. *Neurocomputing* 71, 4–6, 641–647.
- KUMAR, A. AND ZHANG, D. 2005. Personal authentication using multiple palmprint representation. *Pattern Recog.* 38, 10, 1695–1704.
- KUMAR, A. AND ZHANG, D. 2006. Personal recognition using hand shape and texture. *IEEE Trans. Image Process.* 15, 8, 2454–2461.
- KUMAR, A., WONG, D., SHEN, H., AND JAIN, A. 2003. Personal verification using palmprint and hand geometry biometric. In *Proceedings of the 4th International Conference on Audio- and Video-Based Biometric Person Authentication*. Springer, 668–678.
- LATHAUWER, L., MOOR, B., AND VANDERWALLE, J. 2000. A multilinear singular value decomposition. *SIAM J. Matrix Anal. Appl.* 21, 4, 1233–1278.
- LEE, T. 1996. Image representation using 2d gabor wavelet. *IEEE Trans. Pattern Anal. Mach. Intell.* 18, 10, 959–971.
- LEUNG, M., FONG, A., AND HUI, S. 2007. Palmprint verification for controlling access to shared computing resources. *IEEE Pervasive Comput.* 6, 4, 40–47.
- LIU, L. AND ZHANG, D. 2005. Palm-line detection. In *Proceedings of International Conference on Image Processing*. 269–272.
- LI, F. AND LEUNG, K. 2006. Hierarchical identification of palmprint using line-based hough transform. In *Proceedings of the 18th International Conference on Pattern Recognition*. 149–152.
- LI, W., ZHANG, D., AND XU, Z. 2002. Palmprint identification by fourier transform. *Int. J. Pattern Recog. Artif. Intell.* 16, 4, 417–432.
- LI, Y., WANG, K., AND ZHANG, D. 2005. Palmprint recognition based on translation invariant zernike moments and modular neural network. In *Lecture Notes on Computer Science* vol. 3497, 177–182.
- LI, W., YOU, J., AND ZHANG, D. 2005. Texture-based palmprint retrieval using a layered search scheme for personal identification. *IEEE Trans. Multimedia* 7, 5, 891–898.
- LIU, L., ZHANG, D., AND YOU, J. 2007. Detecting wide lines using isotropic nonlinear filtering. *IEEE Trans. Image Process.* 16, 6, 1584–1595.
- LU, G., ZHANG, D., AND WANG, K. 2003. Palmprint recognition using eigenpalms features. *Pattern Recog. Lett.* 24, 9, 1463–1467.
- MAIO, D., MALTONI, D., CAPPELLI, R., WAYMAN, J., AND JAIN, A. 2002a. Fvc2000: Fingerprint verification competition. *IEEE Trans. Pattern Anal. Mach. Intell.* 24, 3, 402–412.
- MAIO, D., MALTONI, D., CAPPELLI, R., WAYMAN, J., AND JAIN, A. 2002b. Fvc2002: Second fingerprint verification competition. In *Proceedings of the 16th International Conference on Pattern Recognition*. 811–814.
- MAIO, D., MALTONI, D., CAPPELLI, R., WAYMAN, J., AND JAIN, A. 2004. Fvc2004: Third fingerprint verification competition. In *Proceedings of the International Conference on Biometric Authentication*. 1–7.

- NANDAKUMAR, K., CHEN, Y., DASS, D., AND JAIN, A. 2008. Likelihood ratio-based biometric score fusion. *IEEE Trans. Pattern Anal. Mach. Intell.* 30, 2, 342–347.
- NIST. 2008. The fbi's next generation identification (ngi). [http://fingerprint.nist.gov/standard/presentations/archives/NGI\\_Overview\\_Feb\\_2005.pdf](http://fingerprint.nist.gov/standard/presentations/archives/NGI_Overview_Feb_2005.pdf).
- NOH, J. AND RHEE, K. 2005. Palmprint identification algorithm using hu invariant moments and otsu binarization. In *Proceedings of the 4th International Conference on Computer and Information Science*. 94–99.
- OJALA, T., PIETIKÄINEN, M., AND HARWOOD, D. 1996. A comparative study of texture measures with classification based on feature distribution. *Pattern Recog.* 29, 1, 51–59.
- OJALA, T., PIETIKÄINEN, M., AND MÄENPÄÄ, T. 2002. Multiresolution gray-scale and rotation invariant texture classification with local binary patterns. *IEEE Trans. Pattern Anal. Mach. Intell.* 24, 7, 971–987.
- PAN, X., RUAN, Q., AND WANG, Y. 2007a. An improved 2d lpp method on gabor features for palmprint recognition. In *Proceedings of IEEE International Conference on Image Processing*. 413–416.
- PAN, X., RUAN, Q., AND WANG, Y. 2007b. Palmprint recognition using fusion of local and global features. In *Proceedings of the International Symposium on Intelligent Signal Processing and Communication Systems*. 642–645.
- PANG, Y., TEOH, A., NGO, D., AND SAN, H. 2004. Palmprint verification with moments. *J. Comput. Graph. Vis.* 12, 1–3, 325–332.
- PHILLIPS, P. 2007. Frvt 2006 and ice 2006 large-scale results. <http://iris.nist.gov/ice/FRVT2006andICE2006-LargeScaleReport.pdf>.
- PHILLIPS, P., MOON, H., RIZVI, S., AND RAUSS, P. 2000. The feret evaluation methodology for face-recognition algorithms. *IEEE Trans. Pattern Anal. Mach. Intell.* 22, 10, 1090–1104.
- PHILLIPS, P., GROTH, P., MICHEALS, R., BLACKBURN, D., TABASSI, E., AND BONE, J. 2003. Facial recognition vendor test 2002 evaluation report. In *Proceedings of the 7th Annual Symposium on Principles of Programming Languages*.
- POON, C., WONG, D., AND SHEN, H. 2004a. A new method in locating and segmenting palmprint into region-of-interest. In *Proceedings of the 17th International Conference on Pattern Recognition*. 533–536.
- POON, C., WONG, D., AND SHEN, H. 2004b. Personal identification and verification: fusion of palmprint representations. In *Proceedings of the European Conference on Biometric Authentication*. 782–788.
- QIN, A., SUGANTHAN, P., TAY, C., AND PA, H. 2006. Personal identification system based on multiple palmprint features. In *Proceedings of the 9th International Conference on Control, Automation, Robotics and Vision*. 1–6.
- RIBARIC, S. AND FRATRIC, I. 2005. A biometric identification system based on eigenpalm and eigenfinger features. *IEEE Trans. Pattern Anal. Mach. Intell.* 27, 11, 1698–1709.
- ROWE, R., ULUDAG, U., DEMIRKUS, M., PARTHASARADHI, S., AND JAIN, A. 2007. A spectral whole-hand biometric authentication system. In *Proceedings of Biometric Symposium*.
- SARKAR, S., PHILLIPS, P., LIU, Z., VEGA, I., GROTH, P., AND BOWYER, K. 2005. The humanoid gait challenge problem: Data sets, performance, and analysis. *IEEE Trans. Pattern Anal. Mach. Intell.* 27, 2, 162–177.
- SCHÖLKOPF, B., SMOLA, A., AND MLLER, K. 1998. Nonlinear component analysis as a kernel eigenvalue problem. *Neural Comput.* 10, 5, 1299–1319.
- SHANG, L., HUANG, D., DU, J., AND ZHENG, C. 2006. Palmprint recognition using fastica algorithm and radial basis probabilistic neural network. *Neurocomputing* 69, 13–15, 1782–1786.
- SHU, W. AND ZHANG, D. 1998. Automated personal identification by palmprint. *Opt. Eng.* 38, 8, 2359–2362.
- SNELICK, R., ULUDAG, U., MINK, A., INDOVINA, M., AND JAIN, A. 2005. Large scale evaluation of multimodal biometric authentication using state-of-the-art systems. *IEEE Trans. Pattern Anal. Mach. Intell.* 27, 3, 450–455.
- SUN, Z., TAN, T., WANG, Y., AND LI, S. 2005. Ordinal palmprint representation for personal identification. In *Proceedings of the International Conference on Computer Vision and Pattern Recognition*. 279–284.
- SWGFAST. 2006. Scientific working group on friction ridge analysis, study and technology. <http://www.swgfast.org/>.
- TEOH, A., NGO, D., AND GOH, A. 2004. Biohashing: Two factor authentication featuring fingerprint data and tokenised random number. *Pattern Recog.* 37, 11, 2245–2255.
- TEOH, A., KUAN, Y., AND LEE, S. 2008. Cancellable biometrics and annotations on biohash. *Pattern Recog.* 41, 6, 2034–2044.

- WANG, M. AND RUAN, Q. 2006a. Palmprint recognition based on two-dimensional methods. In *Proceedings of the 8th International Conference on Signal Processing*.
- WANG, Y. AND RUAN, Q. 2006b. Kernel fisher discriminant analysis for palmprint recognition. In *Proceedings of the 18th International Conference on Pattern Recognition*. 457–460.
- WANG, Y. AND RUAN, Q. 2006c. Palm-line extraction using steerable filters. In *Proceedings of the 8th International Conference on Signal Processing*.
- WANG, Z., BOVIK, A., SHEIKH, H., AND SIMONCELLI, E. 2004. Image quality assessment: From error to structural similarity. *IEEE Trans. Image Process.* 13, 4, 600–612.
- WANG, X., GONG, H., ZHANG, H., LI, B., AND ZHUANG, Z. 2006. Palmprint identification using boosting local binary pattern. In *Proceedings of the International Conference on Pattern Recognition*. 503–506.
- WANG, J., YAU, W., SUWANDY, A., AND SUNG, E. 2008. Person recognition by fusing palmprint and palm vein images based on “Laplacianpalm” representation. *Pattern Recog.* 41, 5, 1514–1527.
- WONG, M., ZHANG, D., KONG, W., AND LU, G. 2005. Real-time palmprint acquisition system design. *IEE Proc. Vis. Image Signal Process.* 152, 5, 527–534.
- WRIGHT, J., YANG, A., GANESH, A., SASTRY, S., AND MA, Y. 2009. Robust face recognition via sparse representation. *IEEE Trans. Pattern Anal. Mach. Intell.* 31, 2, 210–227.
- WU, X., WANG, K., AND ZHANG, D. 2002. Fuzzy directional element energy feature (fdeef) based palmprint identification. In *Proceedings of the 16th International Conference on Pattern Recognition*. 95–98.
- WU, X., ZHANG, D., AND WANG, K. 2003. Fisherpalms based palmprint recognition. *Pattern Recog. Lett.* 24, 15, 2829–2838.
- WU, X., WANG, K., AND ZHANG, D. 2004a. A novel approach of palm-line extraction. In *Proceedings of the 3rd International Conference on Image and Graphics*. 230–233.
- WU, X., WANG, K., AND ZHANG, D. 2004b. Palmprint recognition using directional line energy feature. In *Proceedings of the 17th International Conference on Pattern Recognition*. 475–478.
- WU, X., WANG, K., AND ZHANG, D. 2005. Palmprint authentication based on orientation code matching. In *Proceedings of the 5th International Conference on Audio- and Video- Based Biometric Person Authentication*. 555–562.
- WU, X., WANG, K., AND ZHANG, D. 2006. Palmprint texture analysis using derivative of gaussian filters. In *Proceedings of the International Conference on Computational Intelligence and Security*. 751–754.
- WU, X., ZHANG, D., AND WANG, K. 2006a. Fusion of phase and orientation information for palmprint authentication. *Pattern Anal. Appl.* 9, 2, 103–111.
- WU, X., ZHANG, D., AND WANG, K. 2006b. Palm line extraction and matching for personal authentication. *IEEE Trans. Syst. Man Cybern. Part A* 36, 5, 978–987.
- YANG, J., ZHANG, D., FRANGI, A., AND YANG, J. 2004. Two-dimensional pca: A new approach to face representation and recognition. *IEEE Trans. Pattern Anal. Mach. Intell.* 26, 1, 131–137.
- YANG, J., ZHANG, D., YANG, J., AND NIU, B. 2007. Globally maximizing, locally minimizing: Unsupervised discriminant projection with applications to face and palm biometrics. *IEEE Trans. Pattern Anal. Mach. Intell.* 29, 4, 650–664.
- YAO, Y., JING, X., AND WONG, H. 2007. Face and palmprint feature level fusion for single sample biometrics recognition. *Neurocomputing* 70, 7–9, 1582–1586.
- YOU, J., LI, W., AND ZHANG, D. 2002. Hierarchical palmprint identification via multiple feature extraction. *Pattern Recog.* 35, 4, 847–859.
- YOU, J., KONG, W., ZHANG, D., AND CHEUNG, K. 2004. On hierarchical palmprint coding with multiple features for personal identification in large databases. *IEEE Trans. Circuits Syst. Video Technol.* 14, 2, 234–243.
- YUE, F., ZUO, W., ZHANG, D., AND WANG, K. 2009. Competitive code-based palmprint recognition using fcm-based orientation selection. *Pattern Recog.* 42, 11, 2841–2849.
- ZHANG, D. 2004. *Palmprint Authentication*. Kluwer Academic, USA.
- ZHANG, D. AND SHU, W. 1999. Two novel characteristic in palmprint verification: Datum point invariance and line feature matching. *Pattern Recog.* 32, 4, 691–702.
- ZHANG, L. AND ZHANG, D. 2004. Characterization of palmprints by wavelet signatures via directional context modeling. *IEEE Trans. Syst. Man Cybern. Part B* 34, 3, 1335–1347.
- ZHANG, D. AND ZUO, W. 2007. Computational intelligence-based biometric technologies. *IEEE Computat. Intell. Mag.* 2, 2, 26–36.
- ZHANG, D., KONG, W. K., YOU, J., AND WONG, M. 2003. Online palmprint identification. *IEEE Trans. Pattern Anal. Mach. Intell.* 25, 9, 1041–1050.

- ZHANG, D., LU, G., KONG, W., AND WONG, M. 2005. Online palmprint authentication system for civil applications. *J. Comput. Sci. Technol.* 20, 1, 1–8.
- ZHANG, D., JING, X., AND YANG, J. 2006. *Biometric Image Discrimination Technologies*. Idea Group Publishing, Hershey, PA.
- ZHANG, L., GUO, Z., WANG, Z., AND ZHANG, D. 2007. Palmprint verification using complex wavelet transform. In *Proceedings of the International Conference on Image Processing*. 417–420.
- ZHANG, D., LU, G., LI, W., ZHANG, L., AND LUO, N. 2009. Palmprint recognition using 3-d information. *IEEE Trans. Syst. Man Cybern.-Part C* 39, 5, 505–519.
- ZHANG, D., GUO, Z., LU, G., ZHANG, L., AND ZUO, W. 2010. An online system of multi-spectral palmprint verification. *IEEE Trans. Instrument. Measure.* 59, 2, 480–490.
- ZHANG, D., KANHANGAD, V., LUO, N., AND KUMAR, A. 2010. Robust palmprint verification using 2d and 3d features. *Pattern Recog.* 43, 1, 358–368.
- ZHAO, W., CHELLAPPA, R., PHILLIPS, P., AND ROSENFELD, A. 2003. Face recognition: A literature survey. *ACM Comput. Surv.* 35, 4, 399–458.
- ZHAO, Z., HUANG, D., AND JIA, W. 2007. Palmprint recognition with 2dpca+pca based on modular neural networks. *Neurocomputing* 71, 1–3, 448–454.
- ZUO, W., ZHANG, D., AND WANG, K. 2006a. An assembled matrix distance metric for 2dpca-based image recognition. *Pattern Recog. Lett.* 27, 2, 210–216.
- ZUO, W., ZHANG, D., AND WANG, K. 2006b. Bi-directional pca with assembled matrix distance metric for image recognition. *IEEE Trans. Syst. Man Cybern. Part B: Cybernetics* 36, 4, 863–872.

Received July 2008; accepted April 2010